Biogeosciences

Open Access

EGU

The dominant role of sunlight in degrading winter dissolved organic matter from a thermokarst lake in a subarctic peatland

Flora Mazoyer[1,2], Isabelle Laurion[1,2], and Milla Rautio[2,3]

[1]Laboratoire de limnologie nordique, Centre Eau Terre Environnement, Institut national de la recherche scientifique, Québec, QC, Canada
[2]Centre for Northern Studies, Université Laval, Québec, QC, Canada
[3]Laboratoire des sciences aquatiques, Département des sciences fondamentales, Université du Québec à Chicoutimi, Québec, QC, Canada

Correspondence: Flora Mazoyer (mazoyer.flora@gmail.com) and Isabelle Laurion (isabelle.laurion@inrs.ca)

Abstract. Dissolved organic matter (DOM) leaching from thawing permafrost may promote a positive feedback on the climate if it is efficiently mineralized into greenhouse gases. However, many uncertainties remain on the extent of this mineralization, which depends on DOM lability that is seemingly quite variable across landscapes. Thermokarst peatlands are organic-rich systems where some of the largest greenhouse gas (GHG) emission rates have been measured. At spring turnover, anoxic waters release the GHG accumulated in winter, and the DOM pool is exposed to sunlight. Here, we present an experiment where DOM photoreactivity and bioreactivity were investigated in water collected from a thermokarst lake in a subarctic peatland during late winter (after 6 months of darkness). We applied treatment with or without light exposure, and manipulated the bacterial abundance with the aim to quantify the unique and combined effects of light and bacteria on DOM reactivity at ice-off in spring. We demonstrate that sunlight was clearly driving the transformation of the DOM pool, part of which went through a complete mineralization into CO_2. Up to 18 % of the initial dissolved organic carbon (DOC, a loss of $3.9\,\mathrm{mgC\,L^{-1}}$) was lost over 18 d of sunlight exposure in a treatment where bacterial abundance was initially reduced by 95 %. However, sunlight considerably stimulated bacterial growth when grazers were eliminated, leading to the recovery of the original bacterial abundance in about 8 d, which may have contributed to the DOC loss. Indeed, the highest DOC loss was observed for the treatment with the full bacterial community exposed to sunlight ($5.0\,\mathrm{mgC\,L^{-1}}$), indicating an indirect ef-

fect of light through the bacterial consumption of photoproducts. Dark incubations led to very limited changes in DOC, regardless of the bacterial abundance and activity. The results also show that only half of the light-associated DOC losses were converted into CO_2, and we suggest that the rest potentially turned into particles through photoflocculation. Sunlight should therefore play a major role in DOM processing, CO_2 production and carbon burial in peatland lakes during spring, likely lasting for the rest of the open season in mixing surface layers.

1 Introduction

In northern regions, permafrost soil temperature is slowly increasing in response to climate change (Biskaborn et al., 2019), leading to permafrost thawing that has many consequences on biogeochemical cycles. Thawing affects the morphology of existing water bodies, and generates new ones through soil subsidence and erosion (Vonk et al., 2015b). When previously frozen carbon stocks are mineralized into greenhouse gases, emissions could feed a positive feedback loop (Schuur et al., 2015), making the fate of this large pool of wide interest.

It is well-established that freshwater is a key component of the global carbon budget (Cole et al., 2007), and that carbon dioxide (CO_2) emissions from lakes are tightly linked to organic carbon inputs (Sobek et al., 2005). More recently, northern lakes were shown to be a significant part of the

carbon cycle dynamic (Wik et al., 2016). The widespread thermokarst features created by abrupt thawing of ice-rich permafrost are particularly considered as hot spots of greenhouse gas emissions (e.g., Cory et al., 2013; Matveev et al., 2016). Olefeldt et al. (2016) estimated that peatland thermokarst landscapes cover 8 % of the northern circumpolar permafrost area, and contain 15 % of all organic carbon within the 0–3 m depth soil layer. Future changes in northern peatlands and the fate of these organic carbon stocks under warming thus deserve attention.

Mineralization of dissolved organic matter (DOM) heavily contributes to CO_2 emissions from inland waters (Lapierre et al., 2013; Tranvik et al., 2009), and mainly depends on two processes: bacterial respiration and sunlight oxidation (photooxidation). To estimate the respective shares of these phenomena or their importance at the scale of a lake or a region is a complex task, especially as they can influence each other (e.g., Obernosterer and Benner, 2004) and are constantly changing over space and time (reviewed by Cory and Kling, 2018). Seasonal variations in CO_2 emission rates have been studied in various types of northern lentic ecosystems (Elder et al., 2018; Hughes-Allen et al., 2021; Prėskienis et al., 2021; Sepulveda-Jauregui et al., 2015), underlining the importance of collecting data on a complete annual cycle. Because the summer season offers easier conditions for sampling and instrument handling, most studies of northern lakes have occurred during this period (Block et al., 2019). The long ice-covered winter and the short ice-breaking spring seasons have historically been overlooked by limnologists, although many northern lakes are covered by ice for several months (Hampton et al., 2017). In fact, recent studies demonstrated that carbon dynamics during winter and at ice-break are far from negligible. The review by Denfeld et al. (2018), presenting results on boreal lakes from Scandinavia and North America, evaluated that 17 % of annual CO_2 emissions happened at the ice-break period, while the study from Jansen et al. (2019) reported up to 30 %. These emissions would mainly result from a fast release of gases accumulated under the ice over the winter season, and from DOM photomineralization that is particularly intense in spring (Vachon et al., 2016, 2017). In northern lakes, sunlight was responsible for up to 49 % of DOM mineralization in springtime, in comparison to only 14 % during the open water season (Vachon et al., 2016). The concept of DOM photoreactivity appears to be particularly central to explain these seasonal or temporal differences (Groeneveld et al., 2016; Pickard et al., 2017).

The goal of our study was to experimentally explore the photoreactivity and bioreactivity of late winter DOM collected from a thermokarstic lake located in a subarctic peatland of eastern Canada. This work is a contribution to learning about carbon cycling in lakes particularly rich in organic matter during the critical ice-off transition period, when DOM microbially processed during the winter becomes exposed to sunlight, higher temperature and oxygenation in surface layers. Winter DOM reactivity has been identified as a major knowledge gap in carbon biogeochemistry research (Hampton et al., 2017), and thermokarst lakes in non-yedoma areas are overlooked systems (Vonk et al., 2015b). The objectives of this study were to assess the effects of sunlight on DOM properties, microbial dynamics and carbon biogeochemistry, as compared to dark processing. We hypothesized that sunlight would have a dominant effect on DOM degradation and mineralization after the long subarctic winter, and a positive effect on bacterial metabolism through the phototransformation of aromatic compounds. We tested this through outdoor incubations where DOM properties, CO_2 concentration, bacterial abundance and bacterial production were followed in replicated microcosms over 18 d.

2 Material and methods

2.1 Study site

The study site was located on the eastern shore of Hudson Bay, 8 km southwest of the village of Whapmagoostui-Kuujjuarapik, Nunavik (Quebec, Canada), in the peatland valley of the Sasapimakwananisikw River, hereafter referred as the SAS valley. The historical development of this subarctic palsa site has been reconstructed through paleoecology in Arlen-Pouliot and Bhiry (2005). Peat accumulation on the marine clay bed began shortly after 6000 cal BP and was interrupted in 400 cal BP with the Little Ice Age. During this cooling period, permafrost established on this ombrotrophic bog and caused the uplifting of palsas (round-shaped mounds). Starting about 100 years ago, temperature and precipitation have increased again, leading to permafrost thaw, palsa collapse, and thermokarst lake formation. These black-colored water bodies lay in a peat bog mainly colonized by ericaceous shrubs, semi-aquatic plants such as *Carex aquatilis*, *Sphagnum* sp. and brown mosses (Bhiry et al., 2011). Nowadays, permafrost in the SAS valley underlies less than 2 % of the land surface, and gathers in the core of the scattered palsa mounds (Bhiry et al., 2011). A detailed landscape diagram and picture can be found in Fig. 7 of Vincent et al. (2017).

2.2 Field sampling and in situ measurements

Sampling was carried out between 19 and 24 March 2016 in a thermokarst lake named SAS2A, with an area of 196 m^2 and a maximum depth of 2.8 m (55.225018° N, 77.696580° W). It took place approximately 2.5 months before the complete disappearance of the ice cover (30 May). More information about this well-studied lake, along with a description of the winter sampling campaign, are reported in Matveev et al. (2019). The lake was covered with 0.5 m of snow and 0.6 m of ice, underlain with a water column of about 1.7 m, which was entirely anoxic. At this time of the year the temperature varied between 0.5 °C (immediately below

the ice) and 1.9 °C (bottom). Despite this thermal stratification, DOM properties were similar through the water column: DOC varied between 18.3 and 20.9 $mgC L^{-1}$, the specific ultraviolet absorbance at 254 nm ($SUVA_{254}$) between 6.78 and 6.85 $L mgC^{-1} m^{-1}$, and the absorption slope at 285 nm (S_{285}) between 0.0111 and 0.0105 nm^{-1} (Table S1 in the Supplement). Water for the experiment was collected on 24 March at the surface just below the ice cover, and stored in a 10 L carboy. In situ data demonstrated that this water was representative of the whole water column in terms of DOM properties and nutrients (Table S1).

2.3 Experimental set-up

In this paper we use the term *bacteria* for simplicity, to refer to any heterotrophic planktonic microorganisms affecting the DOM pool with a maximum size of about 3 μm, which may include archaea, phototrophic eukaryotes and small protozoans. On the other hand, cell counts obtained by flow cytometry only comprise cells smaller than about 1 μm (see section on bacterial abundance below). Also, the term *light* used hereafter refers to sunlight wavelengths involved in photooxidation, thus it includes ultraviolet radiation and not only visible wavelengths.

For logistical reasons, the experiment was set up approximately 4 months after the water was collected in the field, on the roof of the INRS in Quebec City (46.812899° N, 71.223821° W in Quebec, Canada). Some DOM changes were noticed between water collection and the beginning of the experiment (see Table S1 to compare with Table 1), where we could observe increases in dissolved organic carbon (DOC, by 15 %) and in fluorescing DOM (by 64 %), along with decreases in chromophoric DOM (by 17 % at 320 nm) and in aromaticity (by 28 %). We assumed these changes to be representative of what is naturally happening in the lake over the long winter as organic matter leaches from particles and DOM and bacteria interact under the ice. Oxygenation at water collection was likely limited as it was done with a thin-layer sampler connected to a peristaltic pump, and SAS2A water was shown to be very resistant to oxygenation (Folhas et al., 2020). The collected water was thus kept under similar conditions as found under the ice (dark, 4 °C, no oxygenation since the container was filled to the top in the field). These physicochemical conditions are structuring this type of ecosystem in winter, where there is no input of fresh DOM that could drive bacterial community or DOM pool changes (Bertilsson et al., 2013). Ultimately, we considered the experimental water to contain a DOM and bacterial community representative of the winter, even after a 4-month delay.

The preparation of the experiment started with series of filtration steps to generate two types of water, one containing the original bacterial community (1.5 μm filtered) and the other with a largely reduced bacterial abundance (0.2 μm filtered). While we tried to achieve a sterile sample, flow cytometry results later indicated that the original abundance was only reduced by 95 %. The filtration steps included prefiltration through 64 and 5 μm sieves using Milli-Q rinsed NITEX®, followed by filtration through precombusted 1.5 μm glass fiber filters (VWR®, nominal porosity) to remove heterotrophic nanoflagellates and non-living particles. The study from del Giorgio and Bouvier (2002) reported that 1 μm glass fiber filters showed good results for that purpose. We observed that filters were brittle during the filtration steps (potentially related to the preburning step), and we suspect that cracks may have existed. Part of this water was kept for the incubation with bacteria, and the rest was subsequently passed through a sterile 0.2 μm capsule filter (HT Tuffryn® polysulfone membrane, Pall Corp.), or after the faster than expected capsule clogging, a double filtration step using precombusted 0.7 μm glass fiber filters (GF75, nominal porosity, Advantec®) and prerinsed 0.2 μm cellulose acetate filters (Advantec®) to remove bacteria. Water filtered by these two methods was merged to obtain a homogeneous 0.2 μm filtrate.

These two types of water were exposed to natural sunlight or dark conditions on the roof of the laboratory during 18 d, from 30 July to 17 August 2016. Five forms of treatment were used involving various combinations of bacteria and light. In four of them, these factors were applied simultaneously: with bacteria and light (hereafter BL), with bacteria in the dark (B), bacteria-filtered with light (L), and bacteria-filtered in the dark (C, for control). The fifth treatment was applied in a consecutive manner: a portion of the bacteria-filtered water was preincubated under natural sunlight for 2 d (approximately 42.6 $MJ m^{-2}$ received in total), and then inoculated with bacteria for an incubation in the dark (PI, for preincubated). The goal of this last treatment was to uncouple the effect of sunlight from the microbial degradation processes. The bacterial inoculation was done using original lake water filtrated through 3 μm polycarbonate filters (PCTE membrane, Advantec®), and using a volumetric ratio of 10 %. The choice of using 3 μm filters (made for logistical reasons) was considered fairly close to using nominal 1.5 μm filters as for B and BL treatments. Overall, the preparation of the experiment lasted about 1 week, during which the water was systematically kept in the dark at 4 °C.

Water incubation was carried out in 60 mL transparent Teflon™FEP bottles (Nalgene™), a material known for its transparency to ultraviolet and visible radiation (above 90 % as shown in Fig. S1 of Logozzo et al., 2021) at the same time of being less fragile to handle than quartz. For each treatment 12 bottles were filled to the rim and incubated allowing triplicate bottles to be sacrificed at days 3, 8, 13 and 18. Dark treatment bottles were wrapped in opaque tape. Bottles were all immersed at the same time in a tray placed on the roof top. The tray was equipped at the bottom with a twisted copper pipe connected to a circulating bath aiming at limiting large increases in temperature during sunny days and tempering day-night differences. The tray was filled with tap

Table 1. Water characteristics at the start of the incubation (T_0), before applying the different treatments: with bacteria and light (BL), with bacteria in the dark (B), bacteria-filtered with light (L), bacteria-filtered in the dark (C), with bacterial inoculum in the dark after a light preincubation (PI). Characteristics include dissolved organic carbon (DOC), dissolved inorganic carbon (DIC), absorption coefficient of DOM at 320 nm (a_{320}), specific absorbance index at 254 nm ($SUVA_{254}$), absorption slope at 285 nm (S_{285}), total fluorescence by DOM (F_{tot} as the sum of the 5 components) and its proportion into C_1–C_5 components, total bacterial abundance (BA), and the bacteria production rate (BP). Variables are given as the triplicate mean ± standard error.

	Water with the original bacterial community[a]	Bacteria-filtered water[b]	Preincubated water inoculated[c]
Associated treatment	BL, B	L, C	PI
DOC ($mgC L^{-1}$)	22.1 ± 0.7	21.9 ± 0.7	19.8 ± 0.2
DIC (mM)	0.32 ± 0.01	0.25 ± 0.01	0.29 ± 0.01
a_{320} (m^{-1})	119 ± 0.2	115 ± 0.5	99 ± 0.9
$SUVA_{254}$ ($L\,mgC^{-1}\,m^{-1}$)	4.68 ± 0.14	4.56 ± 0.13	4.67 ± 0.3
S_{285} (nm^{-1})	0.0100 ± 10^{-5}	0.0100 ± 10^{-5}	0.0110 ± 10^{-5}
F_{tot} (RU)	8.2 ± 0.01	8.2 ± 0.05	6.5 ± 0.02
C_1 (RU, % of F_{tot})	2.8, 34	2.8, 34	2.3, 35
C_2 (RU, % of F_{tot})	2.0, 24	2.0, 24	1.8, 28
C_3 (RU, % of F_{tot})	1.6, 19	1.6, 19	0.9, 14
C_4 (RU, % of F_{tot})	1.2, 15	1.2, 15	1.2, 18
C_5 (RU, % of F_{tot})	0.7, 9	0.7, 9	0.4, 6
BA (10^5 cells mL^{-1})	13.02 ± 2.26	0.69 ± 0.18	1.95 ± 0.26
BP ($\mu gC L^{-1} h^{-1}$)	0.224 ± 0.017	0.003 ± 0.001	0.015 ± 0.001

[a] Filtration with nominal 1.5 μm glass fiber filters to remove most grazers. [b] Filtration with 0.2 μm filters to remove most bacteria (95 %) and all grazers. [c] Prefiltration with 0.2 μm filters for a 2 d incubation under sunlight, followed by the inoculation with 3 μm filtered water at a volumetric ratio of 10 % and incubated in the dark.

water (added daily to offset evaporative losses), and oriented to maximize sunlight exposure, with bottles moved daily to limit unequal shading. Three light and temperature loggers (HOBO Pendant®, ONSET) were installed at the same depth as the bottles to obtain a relative index of incoming sunlight, with one wrapped as in the dark treatment to control for temperature difference among treatments. The temperature in the light averaged 19.7 °C (range 8.5–34.3 °C) as compared to 18.9 °C (8.4–32.0 °C) in the dark (Fig. S1a). These temperatures were higher than the ones measured in SAS2A at the spring ice-break, but averages were similar to temperatures measured at the pond surface in summer (Matveev et al., 2019).

Time zero (T_0 – at day 0) measurements were taken from the three types of water: water containing the original bacterial community (BL and B), the bacteria-filtered water (L and C) and the inoculated preincubated water (PI). They were the only pseudo-replicates from the dataset (i.e., 3 samples taken from the same container, as opposed to 3 replicate bottles for days 3, 8, 13 and 18). At each time step, we measured DOC, dissolved inorganic carbon (DIC), chromophoric dissolved organic matter (CDOM, absorption spectra), fluorescing dissolved organic matter (FDOM, excitation-emission matrices) and bacterial abundance. Bacterial production was only measured at T_0, day 8 and day 18. Note that the filtration steps allowed the water to be oxygenated, so that all treatments at T_0 had an overall mean of 8.96 ± 0.23 $mgO_2 L^{-1}$.

2.4 Incoming radiation during the experiment

Radiation during the incubation was measured every 2 min in a weather station (Wireless Vantage Pro2™ Plus, Davis Instrument Corporation) installed on Laval University campus (http://meteo-laval.gel.ulaval.ca/meteocam-proxy.php, last access: 25 August 2022) at a distance of 5.4 km from INRS (pyranometer integration from 300 to 1100 nm). Missing data during the first 3 d were estimated through a linear regression between the station irradiance and our Pendant logger values. Hourly radiation measured at the SILA station of Whapmagoostui-Kuujjuarapik in 2015 and 2016 (on the shore of Hudson Bay, 8 km away from the study site, pyranometer integration from 300 to 2800 nm; CEN, 2020) were integrated over the incubation period (18 d in August). They were compared to get a sense of incoming sunlight energy at both latitudes (Fig. S1b). Total incoming sunlight energy received in Quebec City (349 $MJ\,m^{-2}$) was 2–13 % higher than sunlight energy recorded at the SILA station (309 and 342 $MJ\,m^{-2}$, depending on the year).

2.5 DIC analysis

The production of dissolved CO_2, as a measure of bacterial respiration and DOM photomineralization, was estimated through changes in DIC concentration, assuming that any increase in DIC over time within the incubation bottles corresponded to a production of CO_2. Exetainer® vials

(12 mL, Labco) were prepared beforehand by adding 120 µL of 10 % HCl, and manually purging with gaseous nitrogen for 1 min. After opening the incubation bottle 3 mL of water was quickly but gently sampled with a syringe and injected with a 21G needle through the septum of a prepared vial. The vial headspace was analyzed by gas chromatography within 2 months (TRACE™ 1310 GC Greenhouse, Thermo Fisher Scientific, Molecular Sieve column 5A 80/100 $6' \times 1/16''$, thermal conductivity and flame ionization detectors, calibration curve made with carbonate solutions 0–2.5 mM). Vials were weighed at each step to convert masses to volumes, and DIC was calculated following Eq. (1) as

$$[DIC] = \frac{[CO_2(g)] \times (V_{vial} - V_{gas} + 1.2 \times V_{gas})}{1.2 \times V_{sample}}, \quad (1)$$

where [DIC] is DIC concentration in mM, $[CO_2(g)]$ the concentration of CO_2 contained into the gaseous phase in mM, V_{vial} the vial volume in mL, V_{gas} the gas volume contained in the vial in mL, and V_{sample} the sample volume added to the vial in mL. The value of 1.2 is the Henry's law volatility constant K_H for CO_2.

2.6 DOM analyses

Water samples were filtered through 0.45 µm polyethersulfone syringe filters (AMD Manufacturing Inc.) and stored in 40 mL glass vials at 4 °C. Part of this water was used to perform the optical analyses within 24 h after sampling, and the rest was stored for later DOC analysis (within 2 months) on a Total Organic Carbon analyzer (Aurora 1030W, O.I. Analytical) using the persulfate oxidation method (precision <5 %, detection limit 0.1 mg L^{-1}).

The CDOM absorbance scans between 200 and 800 nm on samples brought to room temperature were obtained with a dual beam spectrophotometer (2 nm slits, scan speed 200 nm min^{-1}, Cary 100 Bio, Varian) using a 1 cm path quartz cuvette. The null-point adjustment was applied on blank-corrected absorbance spectra using the mean value from 790 to 800 nm, and data were converted to Napierian absorption coefficients (in m^{-1}). The absorption coefficient at 320 nm (hereafter, a_{320}) was used as a proxy for CDOM quantification. The SUVA$_{254}$, calculated following Weishaar et al. (2003), was used as a proxy for the aromatic content of DOM. The spectral slope between 275 and 295 nm (S_{285}, in nm^{-1}), as a linear fit on log-transformed data, was also calculated, commonly used as an indicator of the mean size of DOM molecules (Helms et al., 2008).

Fluorescence excitation-emission matrices (EEMs) were obtained on a spectrofluorometer (Cary Eclipse, Varian) across an excitation waveband from 240 to 450 nm (10 nm increments), and an emission waveband from 300 to 560 nm (2 nm increments). DOM was characterized by the extraction of fluorescent components using the parallel factor analysis (PARAFAC) developed by Stedmon et al. (2003). Blank-subtracted EEMs were corrected for the inner-filter effect using absorbance spectra and standardized to Raman units (RU), after which the Raman and Rayleigh scatter peaks were excised. All preprocessing was done with the FDOM-corr toolbox for Matlab (version 1.4, Murphy et al., 2010), and the model was created using the drEEM toolbox (version 0.1.0, Murphy et al., 2013). Extra samples from another experiment done on the same pond ($N = 54$; unpublished data) were added to the 60 samples of the current experiment in order to obtain a minimum of 100 matrices to generate the PARAFAC model (according to Stedmon and Bro, 2008). A 5-component model was validated using split-half analysis, and the residuals did not present any obvious peak signals.

Fluorescence components C_1–C_5 were expressed as the maximum fluorescence intensity at the peak in RU. The total fluorescence (F_{tot}) was obtained by summing the fluorescence of all 5 components, and used to calculate their relative abundance. The identification of the components was done in the Openfluor database of Murphy et al. (2014) through the selection of similar spectra with a Tucker congruence coefficient (TCC) exceeding 0.95 on the excitation and emission spectra simultaneously. Unfortunately, the EEMs from T_0 could not be exploited (related to an acquisition problem). However, based on CDOM dynamics from T_0 and FDOM dynamics from T_3 (see results), we reasonably estimated the initial values of treatments B, C and PI to be the same as at T_3, and the initial values of BL and L to be similar to the ones of B and C. These values were therefore used to calculate temporal changes and to make statistics hereafter.

2.7 Bacterial abundance and production

Bacterial abundance (BA) was obtained on water samples fixed with glutaraldehyde (1 % final concentration), snap-frozen with liquid nitrogen, and kept at −80 °C until analyzed with a flow cytometer (Accuri C_6 Plus, BD Biosciences). Before counting, the samples were thawed at 4 °C overnight and then brought to room temperature. Cells were stained with SYBR Green I (2.5X final concentration) for 15 min in the dark. Data were acquired at the slowest flow rate, with speed measured daily using Trucount™ absolute counting tubes (mean of 0.43 µL s^{-1} over the analytical period). Yellow-green Fluoresbrite® microspheres of 1 µm diameter (Polysciences Inc.) were added directly to Trucount tubes as an internal size standard and to control gate positions. Cells were discriminated on a log-scale using green fluorescence and forward scatter for blue laser excitation. One acquisition was done for each sample at a maximum rate of 1000 events s^{-1} and with a minimum of 10 000 events counted. Gating was refined considering all samples in order to extract their population abundance using the same gates (Fig. S4). The presence of picophytoplankton cells was checked in samples exposed to sunlight using cytometer runs done without staining with SYBR Green I and looking at fluorescence from chlorophyll-a or phycocyanin, but no population could be discriminated from the noise. Samples were

analyzed before and after sonication (Sonifier® SFX150, Branson™, 30 s with pulses of 0.1 s s^{-1} at 50 % duty cycle, ∼ equivalent to 10 W) to evaluate the relative proportion of particle-attached and free living bacteria. The sonication rod was directly introduced into the acquisition tubes placed in an ice bath.

Bacterial production (BP) was measured using the tritiated leucine incorporation method (Kirchman et al., 1985), with centrifugation improvement proposed by Smith and Azam (1992). Production assays were started less than 3 h after sampling. A working solution with a specific activity of 150 Ci mmol^{-1} was added to triplicate aliquots, each containing 1.2 mL of sample water (final leucine concentration of 30 nM). Incubations for 2 h in the dark at room temperature (∼ 21 °C) were ended with the addition of trichloroacetic acid (TCA, 5 % final concentration). For each triplicate, one additional tube was fixed with TCA at the beginning of the incubation to account for passive incorporation of tritiated leucine by cells. The tracer concentration and incubation duration were based on previous studies on thermokarst lakes near the sampling site (Roiha et al., 2015). Tubes were then stored at −20 °C until analysis. Samples were melted at room temperature, centrifuged for 10 min at 16 000 g, and the pellet rinsed 2 times with 5 % TCA solution. Scintillation cocktail (Ecolite(+)™, MP Biomedicals) was added for at least 24 h before counting with a liquid scintillation analyzer (Tri-Carb® 2910TR, Perkin Elmer). Counts per minute were corrected with controls and converted into disintegration per minute (DPM) using the counting efficiency calculated from home-made standards. Sample aliquots acting as controls were prepared with the same steps described above but without adding the tracer solution, while standards were aliquots with a known amount of radioactive leucine. Calculation details on BP can be found in the Supplement.

2.8 Data analysis

The experimental design was analyzed with ANOVAs excluding T_0 values. Effects and interactions among BL, B, L and C treatments were examined with a 3-way ANOVA testing for light (2 levels, fixed), bacteria (2 levels, fixed) and time (4 levels, fixed) on each variable. PI treatment was not included in this analysis due to its distinct preparation method, but it was compared to the other treatments separately using a 2-way ANOVA testing for treatments (5 levels, fixed) and time (4 levels, fixed). ANOVA assumptions were checked by graphical examination of the residuals plotted against the expected values. Except for C_5, all variables were transformed to validate assumptions of the ANOVA. A log-transformation was applied to S_{285}, while all remaining variables were transformed with square root. When a term of the ANOVA was significant, comparison between the different levels was obtained using Tukey's honestly significant difference post hoc test. The Wilcoxon test was occasionally used to test for two groups mean differences. A significance level of $\alpha = 0.05$ was used for all statistical analysis. The 95 % confidence interval around T_0 values were calculated and represented in the figures as a thin bar on the left side of T_0. Values falling outside this interval during the incubation were considered as significantly different from T_0. ANOVAs were performed with JMP 15.0 software, while the rest of the statistical analyses and graphs were done on RStudio 1.2.5 software.

3 Results

3.1 Initial characteristics of incubated waters

At T_0, DOM properties between waters with or without bacteria were similar, showing that the filtration step did not affect DOM composition (Table 1). As expected, bacterial abundance and production were much higher in the water containing the initial bacterial community, with 19 times more free bacterial cells, and a 75 times higher production rate (BP normalized by BA was also 4 times higher on average). Despite our sterilization efforts relying on 0.2 μm filtration, approximately 70 000 cells per mL remained in the bacteria-filtered water (i.e., 5 % of the original abundance). This implies that L and C treatments were not completely sterile, but this filtration step apparently removed all protists (see below).

The preincubated water (PI treatment) displayed different values for all variables except SUVA$_{254}$ as compared to the two other T_0 water types, which was expected after an exposition to sunlight for 3 d. DOC, a_{320} and F_{tot} were lower than for the two other waters, while S_{285} was higher (Table 1). There had been an increase of DIC during the pretreatment with light (by approx. 16 %) when comparing values with those in bacteria-filtered water from which PI treatment water was prepared (this cannot be seen in Fig. 1 since DIC at T_0 was subtracted from all values). Bacterial abundance and production were also higher in PI than in C treatment, showing the effect of the bacterial inoculation, but remained considerably lower than in the water containing the original bacterial community. The five fluorescent components were less abundant in the preincubated water than in the two other waters. Overall, C_1 and C_2 were the most abundant fluorophore groups (∼ 60 % in total), C_5 was the least abundant (< 10 %), and C_3 and C_4 were approximately present in the same proportions (∼ 15 % each).

All five DOM components were identified as humic-like, with maximum emission peaks above 400 nm (see all supporting references in Table S2 and Fig. S2). C_1 is broadly described as a common ubiquitous group of fluorophores with a terrestrial origin (e.g., Williams et al., 2010). C_2 was most probably of terrestrial origin (found predominantly in wetland and forest drainage waters by Søndergaard et al., 2003) and described as biorefractory. Component C_3 showed the longest and broadest excitation band, along with the longest
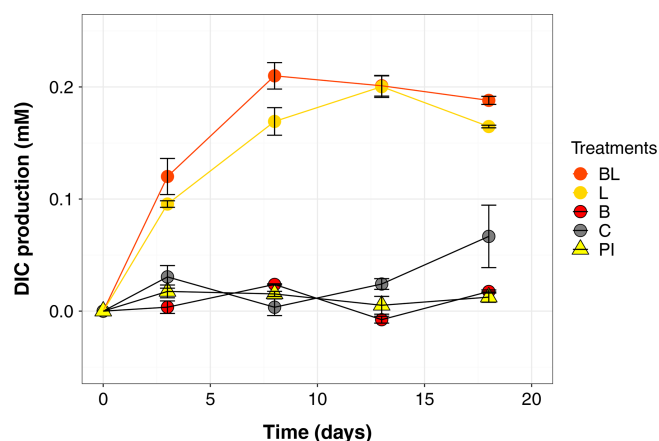
Figure 1. Temporal dynamics in dissolved inorganic carbon (DIC), presented as the difference from the mean value at time zero for each treatment (i.e., the DIC produced during the incubation). Error bars represent the standard errors. Treatments are as follows: water with original bacterial community exposed to light (BL), bacteria-filtered water exposed to light (L), water with original bacteria incubated in the dark (B), bacteria-filtered water incubated in the dark (C), preincubated water inoculated with bacteria and incubated in the dark (PI).

emission peak, suggesting that it belongs to a particularly high molecular weight fraction of terrestrial humic matter (Stedmon et al., 2003). It was reported in very diverse environments and usually assigned to a terrestrial origin (e.g., Osburn et al., 2012), but some studies assigned it to an autochthonous origin. Note that Murphy et al. (2018) demonstrated that humic-like components from terrestrial and autochthonous sources could display similar spectra and chemical characteristics, thus highlighting the uncertainty related to the origin of fluorescing components. Finally, even though the origin of C_4 and C_5 is uncertain, they could be characterized by their photodegradability.

3.2 Changes in chemical and optical variables during the incubation

The largest changes in DIC, DOC and various CDOM properties were observed for the light treatments BL and L (complete ANOVA results presented in Table S3). DIC (Fig. 1) significantly accumulated in bottles in both light treatments until day 8 (post hoc, $P < 0.0001$), at respective rates of 0.025 and 0.020 mM d^{-1}, after which it remained stable (post hoc, $P > 0.97$). Correspondingly, concentrations in DOC and CDOM (Fig. 2, with a_{320} as a proxy for CDOM concentration) significantly decreased with light, with total losses of 6.7 mgC L^{-1} (by 30 %) and 47 m^{-1} (40 %) for BL, and 5.6 mgC L^{-1} (25 %) and 45 m^{-1} (39 %) for L after 18 d of incubation. DIC, CDOM and DOC values were not statistically different between the two light treatments, with the exception of CDOM at day 8 (post hoc, $P < 0.0001$), and DOC at

days 13 and 18 (post hoc, $P < 0.0126$). Significant increases in S_{285} (Fig. 2) were also observed in the light treatments, indicating a decline in DOM overall molecular size over time. There was a significant decreasing trend in SUVA$_{254}$ during the experiment, but values did not get out of the 95 % confidence interval of T_0 (data not shown). As for CDOM, there was an overall decrease in FDOM under light (Fig. 3). After 1 d, F_{tot} losses were 3.6 RU (by 45 %) and 4.1 RU (50 %) for BL and L, respectively. C_1 and C_3 contributed the most to these losses (around 30 % each), followed by C_2 and C_5. C_5 completely disappeared after 13 d of light exposure. On the other hand, C_4 did not vary much but still showed a significant decrease under light exposure. The decreasing dynamic strongly slowed down starting from day 8 for almost all variables.

In contrast to the dynamics observed under sunlight exposure, there were almost no changes over time for the dark treatments (B and C). Only at day 18 was DIC found to be significantly higher in C treatment by comparison to the rest of the incubation, and the DOC value was out of the 95 % confidence interval of T_0 (Figs. 1 and 2). Total DOC losses were 1.5 and 1.7 mgC L^{-1} for B and C treatments, respectively. A sudden increase in all fluorescent components was observed after day 8 (mean increase by 19 %) (Fig. 3). There was no overall difference in the measured variables for B and C treatments, except for DIC, DOC and C_3 fluorescence.

The variables measured in the PI treatment showed responses that were comparable to those of the dark treatments, with limited or no changes in time (Table S4). FDOM components, except C_5, significantly increased after 8 d (post hoc, $P < 0.0004$) in the same proportions as in treatments B and C (mean increase by 19 %). Over 18 d, there was a DOC loss of 1.1 mgC L^{-1} that was not reflected in CDOM (loss < 0.01 m^{-1}). As expected, initial DOM properties in PI treatment such as DOC, a_{320}, S_{285} or C_1 were close to day 3 values of L treatment since the preincubation with light lasted about 3 d (post hoc, $P > 0.30$ at day 3).

3.3 Bacterial abundance (BA) and production (BP)

The BA at T_0 already indicated that sterility was not achieved by the 0.2 µm filtration step (Table 1), and this initial population significantly increased in abundance over time in both L and C treatments (39 and 4 times more at day 18 compared to T_0, respectively; Fig. 4). The most outstanding dynamic was obtained for the L treatment, with an overall growth of 1.5×10^5 cells mL^{-1} d^{-1}. This means it took about 8 d for BA in the 0.2 µm filtered L treatment to reach the initial abundance observed in B and BL treatments, and by the end of the experiment, BA had reached 2.69×10^6 cells mL^{-1}. The bacterial population that bypassed the 0.2 µm filtration, or was airborne during filling the bottles, grew at a much slower pace in the control treatment (0.1×10^5 cells mL^{-1} d^{-1}), and declined after day 13. The BA was stable in treatments with the original bacterial community (BL and B), with values still
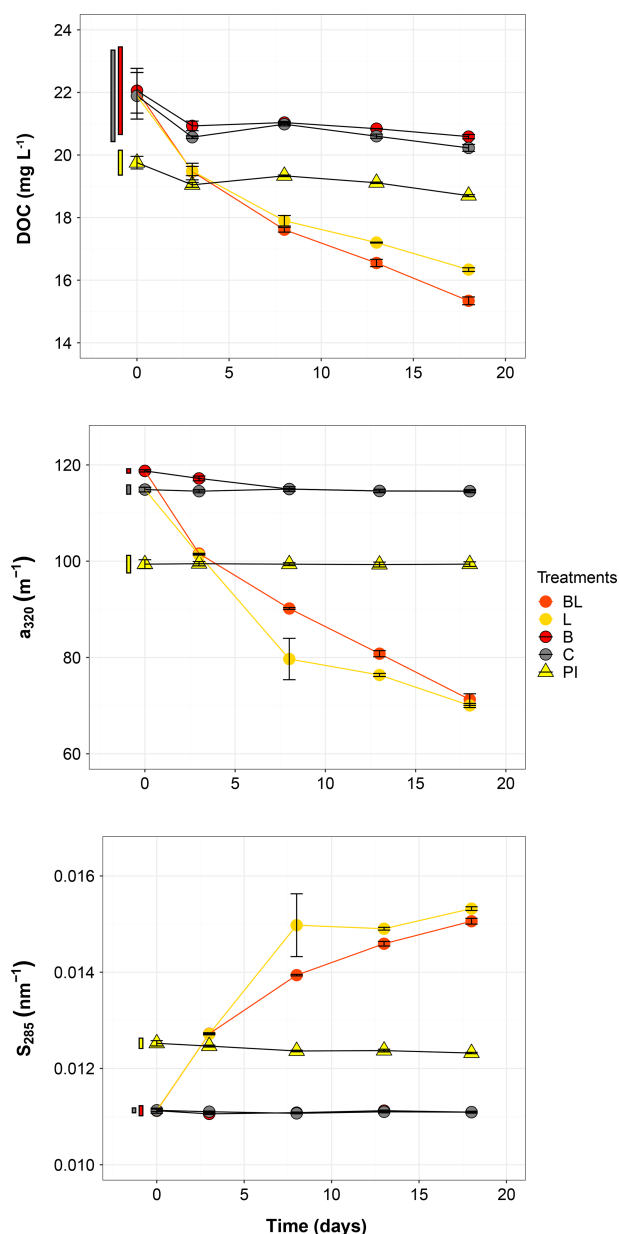
Figure 2. Temporal dynamics of the dissolved organic carbon (DOC), the absorption coefficient at 320 nm (a_{320}) and the absorption slope at 285 nm (S_{285}) for the five treatments. Error bars represent the standard errors. The thin bars on the left of T_0 values indicate the 95 % confidence interval at T_0 for the three water types: 0.2 μm filtered (gray); 1.5 μm filtered (red); 0.2 μm filtered, pre incubated for 3 d and inoculated with bacteria (yellow). Refer to Fig. 1 and Table 1 for the definition of treatments and water types.

inside the 95 % confidence interval of T_0 at day 18. However, bacteria remained overall more abundant in BL than in B treatment (post hoc, $P < 0.0001$). Growth in PI treatment was significant but BA remained stable between day 3 and day 18. At the end of the incubation, there were more bacteria in PI than in C (post hoc, $P = 0.04$).

Bacterial production significantly increased from T_0 in all treatments during the incubation (Fig. 5). The highest production rates were obtained for the BL treatment, reaching 1.11 μgC L^{-1} h^{-1} by the end of the incubation, equivalent to twice the production in the dark (B treatment) at the same moment. The exposure to sunlight and the presence of the initial community both contributed to the higher BP (Table S3). However, for treatments with a large reduction of the original bacterial abundance (L and C), the BP at day 18 was lower than at day 8 (post hoc, $P = 0.04$), which is particularly evident for the L treatment. For PI treatment, BP did not change significantly between day 8 and day 18 (post hoc, $P = 0.9957$). The normalization of BP by the bacterial abundance brought up another perspective to these data (Fig. 5). Exposure to sunlight was no longer a significant factor, and differences between treatments appeared smaller, especially at day 8 where the differences in BP were not significant (post hoc, $P > 0.09$). Nevertheless, it can be noted that the only treatment showing a continuously increasing trend was BL.

3.4 Carbon losses and gains during the experiment

Assessment of the carbon balance allowed to check whether the measured processes (DIC production, bacterial growth) were enough to describe the carbon transfers occurring in the incubation bottles (Fig. 6). In all treatments and at all times, the measured carbon loss (as a decrease in DOC) was always higher (+58 % to +1214 %) than the measured carbon gain (as the sum of DIC and BP), even after maximizing BP in the calculation (i.e., by applying the highest rate obtained to all time periods of any specific treatment). BP gains thus represented on average 10 % and 38 % of the total gain measured, respectively, for the light treatments (BL and L), and for the dark treatments (B, C and PI). Also, the uncertainty around the loss term was generally much higher than around the gain term (mean of 1.06 against 0.15 mgC L^{-1}). However, the difference between losses (in DOC) and gains (in DIC and bacterial biomass) was clearly larger for the two light treatments: on average 3.6 mgC L^{-1} after 18 d of incubation, as compared to 0.8 mgC L^{-1} for the three other treatments (Fig. 6f, Wilcoxon test, $P < 0.0004$). Moreover, BL and L were characterized by a unique pattern in which carbon losses kept increasing, while carbon gains apparently reached a plateau from day 8.

4 Discussion

4.1 Sunlight as a driver of DOM mineralization

One of the main results of this study is the clear dominance of sunlight as a driver of DOM degradation and mineralization in the studied peatland thermokarst lake at the end of winter. In BL and L treatments, the same significant concurrent changes were observed: CO_2 was produced while DOC,
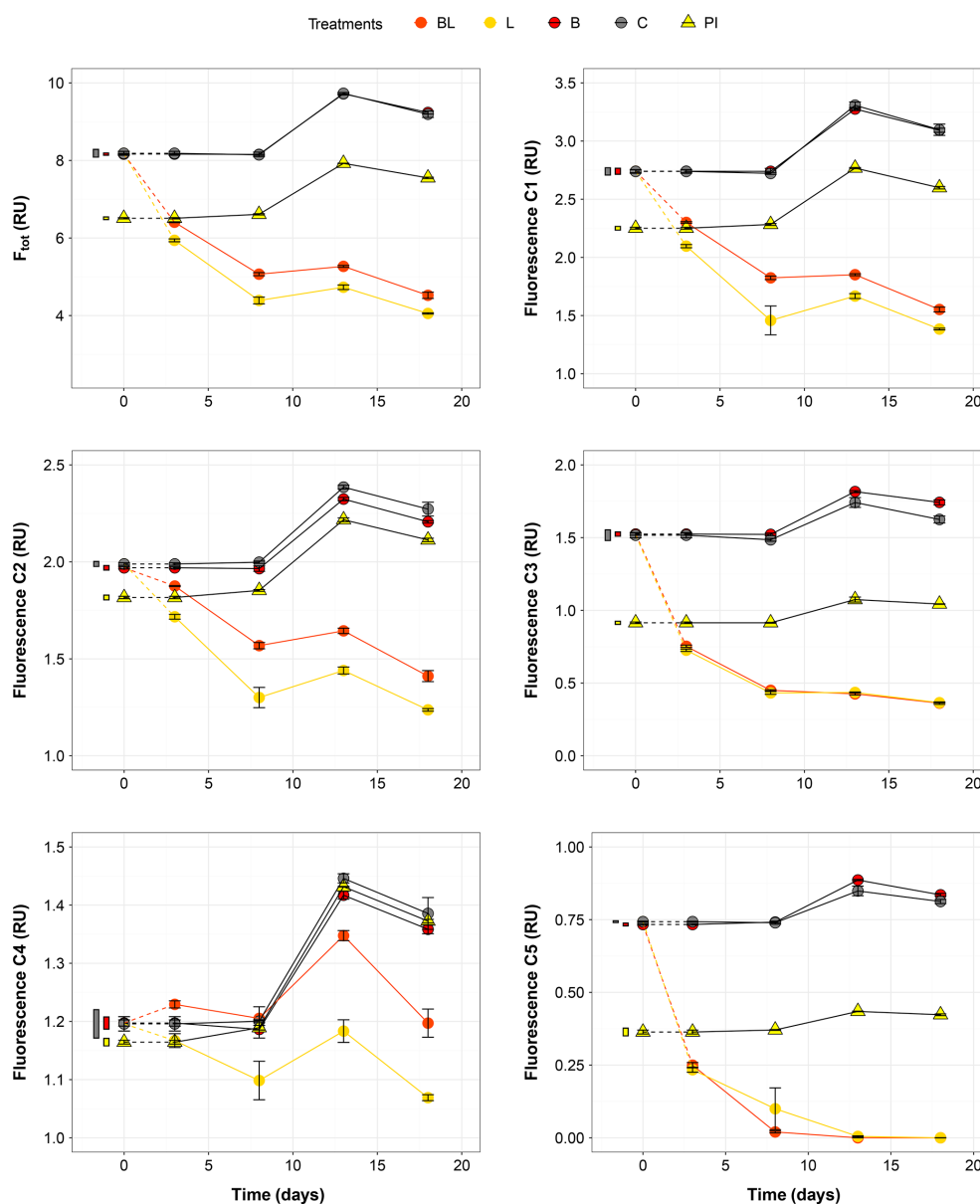
Figure 3. Temporal dynamics of the total fluorescence (F_{tot}) and the five fluorescing components (C_1–C_5) over the 18 d of incubation for the five treatments. Error bars represent the standard errors. The thin bars on the left of T_0 values indicate the 95 % confidence interval at T_0 for the three water types. Dotted lines indicate that T_0 values were extrapolated (see "Material and methods"). Refer to Figs. 1 and 2 and Table 1 for the definition of treatments and water types.

CDOM and FDOM aromatic fractions declined, along with a general decrease in DOM molecular weight (increase of S_{285}). These changes were limited or absent in dark conditions.

Light absorption by CDOM cause a destruction of the chromophores. Optically, this translates into bleaching and the breakage of high molecular weight molecules (Helms et al., 2008; Moran et al., 2000). When this photon-mediated oxidation is complete, CO_2 is produced and a corresponding carbon loss is going from DOC to the gaseous state (Granéli et al., 1996). When the oxidation process is incomplete, various moieties with different stages of oxidation accumulate in water, and their transformation does not result in DOC loss (e.g., Ward et al., 2014). The experiment here shows that both types of reactions occurred. About 4 mgC L^{-1} were lost over 18 d through the direct action of sunlight (L treatment minus C, DOC loss rate of 0.22 mgC L^{-1} d^{-1}). A certain fraction of this loss was certainly generated by the unexpected growth of bacteria in the L treatment; however, a much larger fraction of this loss was likely due to direct photomineralization
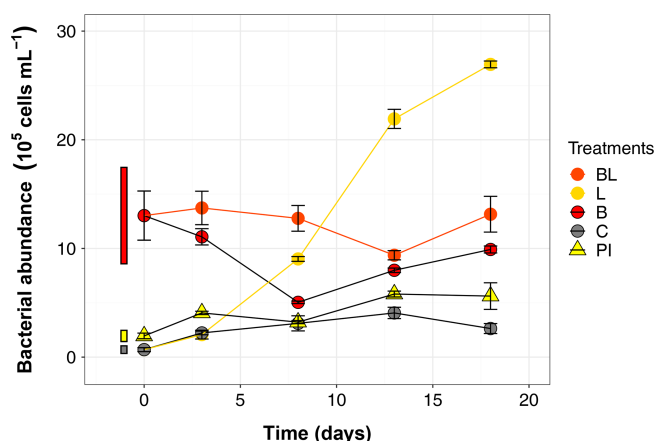
Figure 4. Bacterial abundance over the 18 d incubation for the 5 treatments. Error bars represent the standard errors. The thin bars on the left of T_0 values indicate the 95 % confidence interval at T_0 for the three water types. Refer to Figs. 1 and 2 and Table 1 for the definition of treatments and water types.

Figure 5. Bacterial production without **(a)** and with **(b)** normalization to cell abundance over the incubation period for the five treatments. Error bars represent the standard errors. The thin bars on the left of T_0 values indicate the 95 % confidence interval at T_0 for the three water types. Refer to Figs. 1 and 2 and Table 1 for the definition of treatments and water types.

for two reasons. First, the DIC production was the highest over the first 3 d ($0.38\,\mathrm{mM\,d^{-1}}$) when bacterial regrowth was still minor. Second, when using the highest BP rate measured in the L treatment ($0.54\,\mathrm{\mu gC\,L^{-1}\,h^{-1}}$, measured at day 8), we estimate that a maximum of $0.23\,\mathrm{mgC\,L^{-1}}$ could have been lost through this biological pathway over the incubation period, representing about 6 % of the DOC loss in L treatment. By comparison, $5\,\mathrm{mgC\,L^{-1}}$ were lost in the BL treatment (after subtraction of C treatment, DOC loss rate of $0.28\,\mathrm{mgC\,L^{-1}\,d^{-1}}$). The difference between BL and L treatments can be attributed to the indirect action of sunlight favoring the bacterial consumption of DOC through the production of partially photooxidized biolabile substrates (at a conservative rate of $0.06\,\mathrm{mgC\,L^{-1}\,d^{-1}}$). Overall, we can consider that most DOC lost in BL treatment was triggered by sunlight, with a maximum of 78 % resulting from its direct action (such as full photoconversion into CO_2) and a minimum of 22 % resulting from its indirect action (such as bacterial consumption of photoproducts). The DOC loss in BL and L treatments measured over 18 d represented 23 % and 18 %, respectively, of the initial DOC concentration. We systematically subtracted the DOC loss of the C treatment, considering it would include all DOC losses unrelated to light or bacteria (e.g., through adsorption or dark flocculation: see below). Even if there was a slight regrowth of bacteria also in this control treatment, we considered it negligible as there was no measurable DIC production, and the maximum amount of carbon allocated to bacterial production over the incubation period was estimated at $0.05\,\mathrm{mgC\,L^{-1}}$ (using a BP of $0.11\,\mathrm{\mu gC\,L^{-1}\,h^{-1}}$, measured at day 8), representing less than 1 % of the DOC loss in BL treatment.

We expect DOM from northern peatland thermokarst lakes to be very sensitive to sunlight degradation, at least at icemelt. Other studies on boreal waters support this result. For
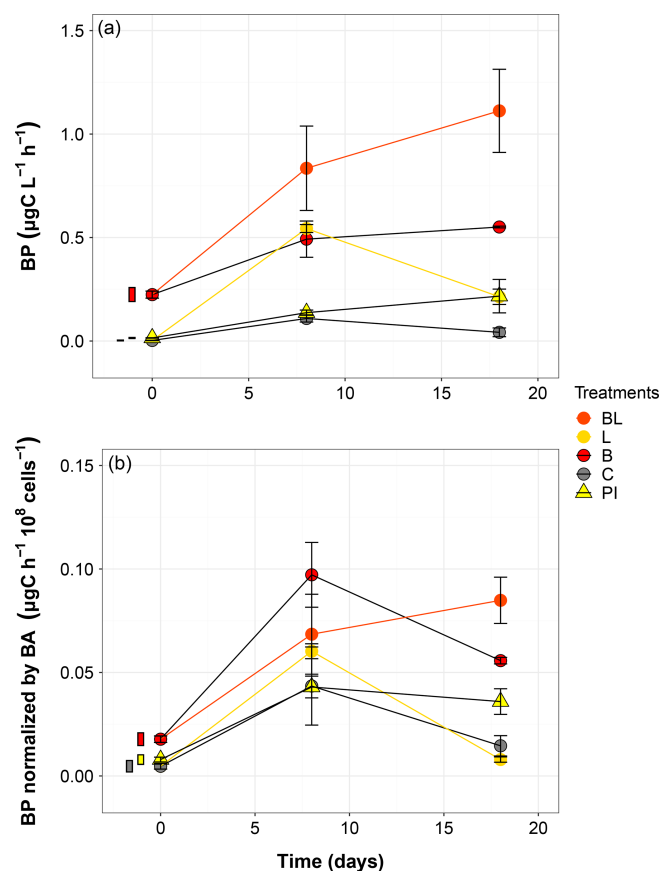
example, the integrated CO_2 photoproduction was 3.5 times larger in spring than in summer for three boreal lakes (Vachon et al., 2016). However, Shirokova et al. (2019), who incubated DOM from a Russian frozen peatland network reported the absence of measurable DOC loss over 1 month of sunlight exposure, and attributed this result to a dominance of refractory allochthonous DOM from soil and peat in this region. Laurion et al. (2021) similarly observed that DOM from organic-rich Arctic tundra ponds was poorly photomineralized, even though it was bleached. These differences suggest a variability in peatland DOM reactivity among regions, potentially related to different historical processing of the organic matter and thus, different molecular assemblages in DOM pools. Historical processing could differ prior to permafrost inception (Tank et al., 2020), or prior to sampling (Laurion et al., 2021). Also, the sunlight dose received (historical dose in situ, or during an experiment) needs to be strictly taken into account when comparing studies. For instance, a major difference between Shirokova et al. (2019)
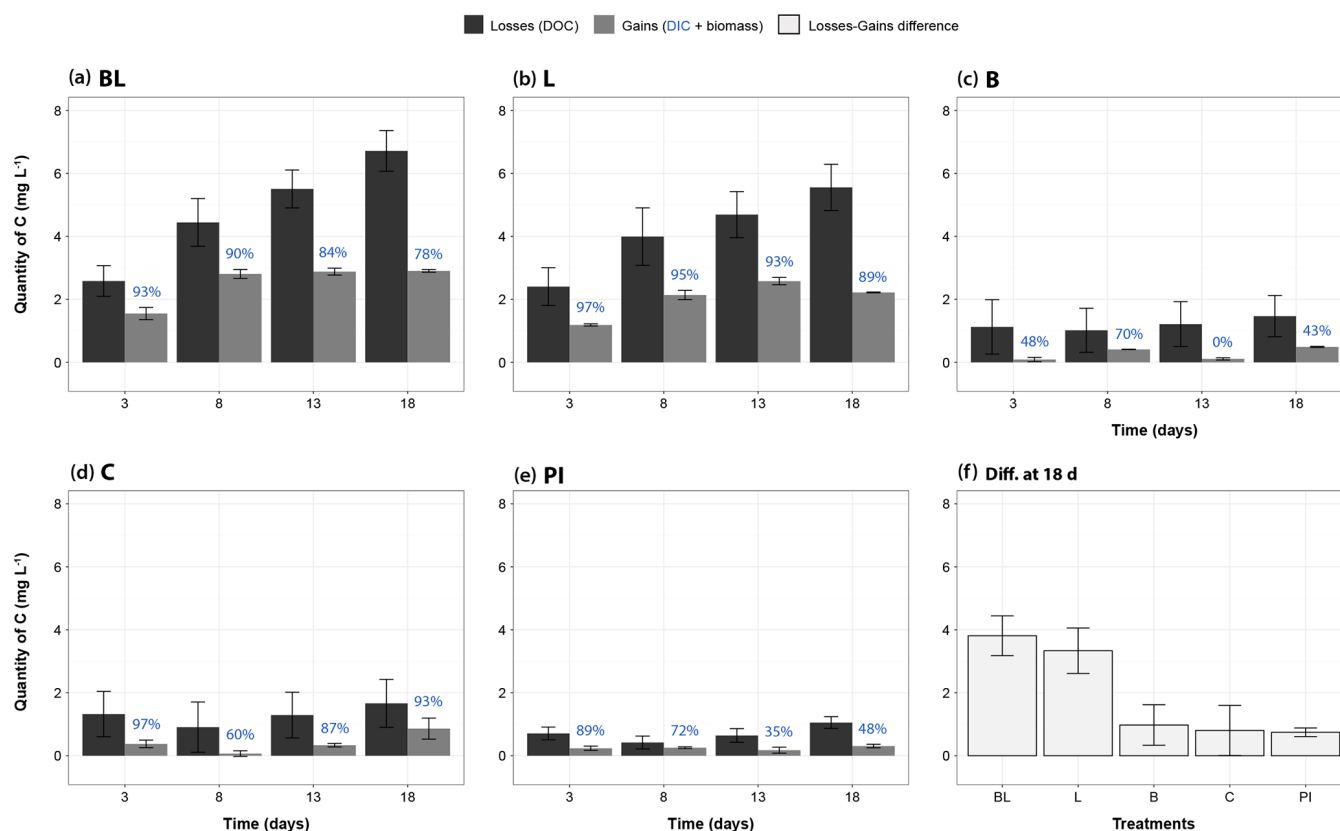
Figure 6. Mass balance of measured carbon transfers during the incubation, categorized as "losses" and "gains". Panels **(a)**– **(e)** correspond to treatments BL, L, B, C and PI, respectively, and present the mass changes of carbon relative to T_0 for days 3, 8, 13 and 18. Black bars represent the DOC losses (through sun mineralization, bacterial consumption, plus all other processes not directly measured), and gray bars represent gains of carbon as the sum of carbon increases in DIC and bacterial biomass. The proportion of gains as DIC is indicated in blue, above the bars. The bacterial biomass carbon gains were estimated for each time period using the highest BP value obtained for each treatment in order to evaluate the maximum potential carbon transfer into bacterial biomass. The panel **(f)** summarizes the difference between losses and gains for each treatment at the end of the incubation, potentially representing DOC flocculation but also other unmeasured processes like DOC conversion into carbon monoxide for the light treatments (see "Discussion"). Error bars represent the standard errors. Refer to Fig. 1 and Table 1 for the definition of treatments.

and our experiment is related to the season when water was collected (late winter vs. peaking summer), which likely has a strong impact on photoexposure history and thus on DOM photolability. Seasonal variations have to be further quantified to make more accurate predictions on the effects of winter contraction associated to climate warming.

4.2 The potential role of flocculation in the DOC loss

In our experiment, DOC losses under sunlight were not fully recovered in the form of DIC or bacterial biomass, and the relative gap between carbon losses and gains was increasing over time (Fig. 6). After 18 d, no more than 51 % of the DOC losses were actually recovered in the form of DIC (from direct photomineralization and photostimulated bacterial respiration), which corresponds to about only 10 % of the initial DOC concentration. This necessarily implies the existence of other light-mediated processes. Part of the unaccounted DOC

loss could have been transformed into carbon monoxide (not measured in the present study), another common photoproduct that depends on the presence of certain DOM aromatic groups (Mopper et al., 2015; Stubbins et al., 2008), although this production would be low (a 1:15 ratio to DIC) according to Moran and Zepp (1997). Most importantly, the natural formation of flocs of organic matter (flocculation) could explain this gap. Several studies showed that sunlight is a triggering factor for the formation of particles and colloids, particularly in CDOM and iron-rich waters (Gao and Zepp, 1998; Helms et al., 2013; Mopper et al., 2015; Oleinikova et al., 2017; von Wachenfeldt et al., 2008). For example, von Wachenfeldt et al. (2008) reported that the synthesis of particulate organic matter from DOC of a sphagnum-dominated mire water almost reached $0.3\,\mathrm{mgC\,L^{-1}\,d^{-1}}$. It has also been shown that rising temperature can favor the transformation of DOC to flocs (Porcal et al., 2015; von Wachenfeldt et al., 2009). We indeed observed particles in filtered water bottles but did not

account for them quantitatively. In summary, photoflocculation was likely occurring in our experimental water, which presented high DOC, CDOM and iron concentrations (Table S1) and was subject to high temperature peaks during the incubation (Fig. S1). Nevertheless, we cannot exclude that two technical issues leading to losses of the CO_2 produced could have also played a role in the gap between DOC loss and DIC gains: (1) dissolved CO_2 turned into gas phase and escaping when the incubation bottles were opened to collect DIC, although air bubbles were very small (1–2 mm in diameter), and (2) the storage delay of exetainer vials exceeding what was recommended by Faust and Liebig (2018).

The DOC loss under B treatment (bacteria and putative small grazers, $1.5\,\mathrm{mgC\,L^{-1}}$) was similar to the one in the control treatment (5 % of initial BA and no grazers, $1.7\,\mathrm{mgC\,L^{-1}}$), suggesting that in the absence of sunlight, carbon losses were not associated to bacterial activity. In fact, the similar gaps between carbon losses and gains in B and C treatments (Fig. 6, not showing a specific temporal trend) could be attributed to the adsorption of DOM molecules onto bottle walls (potentially quicker than flocculation). Helms et al. (2013) experimentally estimated that such adsorption was responsible for the loss of up to $0.08\,\mathrm{mgC\,L^{-1}\,d^{-1}}$ (on 550 mL quartz bottles). They also reported that this phenomenon was apparently strengthened by sunlight exposure, so this potential adsorption may have been even stronger in BL and L treatments. At last, bacteria-mediated flocculation could also have happened during dark incubations. This has been observed in water from oligotrophic boreal lakes in winter, where the bacterial activity would have favored the formation of detrital flocs from CDOM (von Wachenfeldt et al., 2009).

Our results suggest that flocculation may be important in peatland thermokarst lakes, and thus play a critical role in carbon burial. This has been highlighted as a main topic of interest related to the future of aquatic ecosystems affected by thawing permafrost (Vonk et al., 2015b). Flocculation should be systematically quantified during experimental assays testing the role of sunlight in carbon cycling. Other studies corroborate the idea that boreal lakes could be strong carbon sinks through sedimentation processes, especially in ecosystems with high allochthonous humic DOM (Guillemette et al., 2017; von Wachenfeldt and Tranvik, 2008).

4.3   DOM biodegradation and bacterial dynamics in the dark treatments

The quantitative and qualitative changes of DOM in dark treatments were insignificant and comparable among B, C and PI treatments (Fig. 2), despite different bacterial community size and activity, notably between B and the two other treatments (Figs. 4 and 5). The data suggest that late winter DOM was refractory to biodegradation, at least over the incubation period and despite the oxygenation and temperature increase generated by the experimental set-up. Communities were active in these treatments (BP > 0 and modest bacterial growth), but the insignificant DOC loss generated suggests a negligible consumption of carbon through bacterial growth and respiration (CO_2 production could not be detected). However, it is unclear what part of the DOM sustained bacterial activity as CDOM did not change much (except for the small loss of CDOM observed in B treatment over the first 8 d, concurrent to an increase in BP; Figs. 2 and 5). This is different from the results reported by Vonk et al. (2015a) for large streams and rivers, where biodegradation rates were relatively higher in winter than in summer, attributed to shifts in carbon sources and shorter hydrologic residence time in soils. However, there is a difference between lotic and lentic ecosystems in their connectivity with the landscape during winter, that is likely driving this difference in biodegradation. Moreover, it is possible that winter DOM would be biodegraded over longer time scales. For example, Vähätalo and Wetzel (2008) reported that wetland-origin DOM, apparently biorefractory over 1 d, was actually reduced by half over 2.5 years of dark incubation. The importance of degradation over longer time scales becomes relevant in water bodies that have long residence times, such as ponds.

Overall, we cannot exclude that the pre-experimental delay of 4 months could have further depleted the DOM pool of any labile material left at the end of a long winter, or modified the original bacterial community. Indeed, the temperature difference between water under the ice cover in March (0.5–2 °C according to Matveev et al., 2019) and the storage cold chamber (4 °C) could have been enough to stimulate the bacterial consumption of DOM. Bacterial activity is widely influenced by temperature, even by small differences (see Adams et al., 2010 and references therein). Nevertheless, the absence of a DOC decline between water collection and T_0 of the experiment (Tables S1 and 1) supports the fact that DOC was recalcitrant to bacterial consumption, as observed during the experimental incubation in the dark. Actually, the DOC increased during storage, likely caused by natural or bacterial-triggered leaching from particles and colloids in the water, stored unfiltered. The largest change observed during water storage was the production of FDOM, which has also been observed during the experimental incubation, and which we attributed to bacterial DOM transformation (see later). The reasons for CDOM and $SUVA_{254}$ declines are unclear but could both result from bacterial activity and preferential flocculation of the chromophoric fraction. More generally, it is possible that bacterial degradation in winter could be preferentially linked to the particulate fraction of organic matter, which was filtered out prior to the experiment. Free living and particle-associated bacterial communities have indeed been shown to follow distinct seasonal patterns (Rösel et al., 2012). Therefore, it is possible that bacterial consumption of DOM in the 1.5 µm filtered treatment (B) was underestimated both because of this 4-month delay and the removal of particles.

From an ecological perspective, the recalcitrance of late winter DOM to biodegradation in this thermokarst lake is not surprising. It means that the system, at that period, would mainly concentrate molecules at the lower end of the reactivity continuum described by Mostovaya et al. (2017). This is supported by the initial properties of this DOM pool, strongly dominated by aromatic compounds with a typical terrestrial signature (high $SUVA_{254}$ and CDOM, only humic-like FDOM components with allochthonous features). As winter goes by, water gets more depleted in labile material, consumed first and foremost, while fresh inputs of carbon are impeded by the ice cover, the frozen surrounding soil, and the absence of primary production in the lake and on land (Deshpande et al., 2016; Przytulska et al., 2016; Shirokova et al., 2021). Overall, this is consistent with studies on peatland and organic-rich wetland, generally reporting low bacterial growth efficiencies or low microbial DOM processing (i.e., Berggren et al., 2007; Laurion et al., 2021; Shirokova et al., 2019). By comparison, bacterial activity is clearly higher when supplied with fresh plant leachates (Shirokova et al., 2021). The abundance of low-quality substrates in peatland water may be related to the dominance of sphagnum mosses at the study sites. These mosses are known to produce litter of poor organic matter quality that decomposes slowly because their chemical structure holds large concentrations of phenolic, nonpolar and antimicrobial compounds (Turetsky, 2003).

Despite the absence of DOM consumption, microbial communities were relatively active and growing in the dark (Figs. 4 and 5). For example, the normalized BP in the B treatment was particularly high at day 8, and the BA substantially increased from T_0 in PI and C treatments. Dark treatments were also characterized by a notable increase in the signal of all fluorescent components, starting after 8 d of incubation (Fig. 3), just like what was observed during the pre-experimental delay (Tables 1 and S1). This increase presumably happened also in the light treatments BL and L, noticed in the slowing declines of fluorophores (sometimes, even a small increase). Bacteria can produce FDOM, and this has been broadly observed in boreal and arctic lakes (e.g., Berggren et al., 2020; Laurion et al., 2021). The study of Berggren et al. (2020) on 101 boreal lakes suggests the reciprocal dependence between microbial processes and DOM optical properties. Considering the concurrent increase in BP and FDOM, we assume that bacteria were responsible for this synthesis of fluorescent molecules (similar assumption made in Logozzo et al., 2021, for example). The five humic components identified here had mostly been described as terrestrial, but our results suggest that they could also be produced by aquatic bacteria (although in a lake strongly influenced by eroding soils). It is interesting to note that there was no parallel increase of CDOM (a_{320} decreased), suggesting that chromophoric nonfluorescent DOM would have been transformed into FDOM. Overall, bacteria have likely transformed DOM into different types of molecules (production of FDOM and potential other metabolic by-products) instead of strictly consuming it (that would have translated into a DOC decrease).

Lastly, it should be noted that the BP measured in the dark treatments is probably not representative of in situ late winter production, where anoxia prevails and water temperature is close to $0\,°C$. The experimental water was oxygenated during the filtration steps and the temperature regularly peaked around $30\,°C$ during the incubation (Fig. S1), exceeding the maximum temperature reached in situ in summer ($18\,°C$ at the surface, Matveev et al., 2019). The bacterial production reported here was similar to that measured from the same lake in summer (Deshpande et al., 2016), while studies on other thermokarst lakes of the region found strong differences between summer and winter production (Roiha et al., 2015). Nevertheless, our results suggest that the bacterial metabolism was more limited by the quality of DOM than by the environmental conditions (see later), in accordance with results from Bižić-Ionescu et al. (2014) who showed that carbon rather than temperature was the limiting factor on bacterial growth in a temperate oligotrophic lake in winter.

4.4 The photochemical stimulation of bacteria

The exposure to sunlight had a positive impact on the bacterial dynamics of this thermokarst lake, such as noted for ice-wedge trough ponds in the High Arctic by Laurion et al. (2021). On one hand, when only a small proportion of the initial bacterial community was left ($\sim 5\,\%$, L treatment), sunlight exposure induced the exponential growth of these few bacteria, reaching about 10 times the abundance in the dark by the end of the incubation (C treatment; Fig. 4). The BP also increased in the first week but dropped at the end of the experiment (no measurements between days 8 and 18; Fig. 5), possibly indicating that this population was reaching a stationary phase in response to a decline in the photoproduction of high-quality substrates, expressed as a slowing rise in BA. On the other hand, sunlight induced a more persistent rise in BP for BL treatment, although the difference in BP was apparently linked to differences in population size (see normalized BP, Fig. 5b). Yet, the increase in BP did not translate into rising biomass in this treatment. This could be explained by the grazing pressure exerted on bacteria by small protists that were able to pass through the nominal $1.5\,\mu m$ filtration step. Nutrient enrichment experiments realized on summer water from the same lake also showed that BP was maintained or increased while BA dropped (Deshpande et al., 2016) suggesting an important top-down control of bacterial populations in this lake (Bégin and Vincent, 2017; Przytulska et al., 2016). Complex mechanisms involving the viral population could also control the size of the bacterial community facing important changes such as in spring. Girard et al. (2020) demonstrated that communities in SAS2A lake were active and seasonally shifting in response to the population dynamics of host organisms. Interestingly,

this potential viral control would not have acted on the rising population observed in L treatment, potentially linked to the inhibiting action of UV radiation on viral activity.

The observed intensification of protein and cell synthesis under sunlight exposure indicates a photochemical conversion of part of the DOM into substrates readily available for bacterial growth, as previously described in the literature (e.g., Moran and Zepp, 1997). Most common photoproducts are organic acids, but other low molecular weight compounds containing essential nutrients could also be involved (Pullin et al., 2004; Vähätalo et al., 2003; Wetzel et al., 1995). For example, Xie et al. (2012) reported the photoproduction of ammonium from DOM. The higher BP in BL treatment clearly indicates that the bacterial community was benefiting from the photoproduction of essential compounds. However, the insignificant difference in DIC production between BL and L treatments, especially between 0 and 3 d when the BA in L was still negligible, suggests that most CO_2 was directly photoproduced and not resulting from respiration of this fast-growing population.

Results also suggest that the initial sunlight exposure of 2 d in PI treatment was not sufficient to substantially stimulate microbial metabolism. The fact that the initial community was small (inoculum) is not likely to be the reason, because L treatment demonstrated that the initial size of the community was not a strong determinant of its activity in the following days. We hypothesize that the limiting factor was rather the limited amount of photolabile compounds produced over the 2 d of sunlight pre-exposure. CDOM decreased by 14 % and S_{285} increased by 10 %, indicating that photodegradation happened (Table 1), but photoproducts may have been consumed rapidly and the stimulation turned down as soon as the water was placed back in the dark. The superposition of C and L curves in the first 3 d could also indicate that a minimum length of sunlight exposure was needed to produce a boosting effect on bacteria. This lag could reflect the adaptation time needed by the community to respond to a change in the quality of the carbon resource. Ward et al. (2017) demonstrated that shifts in substrate availability were driving deep shifts in bacterial gene expression and composition, translating into time lags in bacterial metabolism. These effects would be occurring in a water column intermittently mixing, generating a complex DOM pool containing molecules photodegraded to various degrees (Matveev et al., 2019).

Achieving sterility is a difficult task and we argue that BA should always be controlled in such experiments (Logozzo et al., 2021 and references therein). Not considering this could lead to interpretation biases. Filtration artifacts can impact short-term biolability assays through their effects on bacterial abundance, composition and predation as demonstrated for waters draining from peatlands in the Netherlands (Dean et al., 2018). Although we achieved a reduction of the initial BA by 95 % in L treatment, it took about 8 d for these bacteria to overtake the abundance observed in BL treatment. Although the effect of sunlight could not be isolated

completely, the experiment clearly demonstrated the efficient role of sunlight on bacterial growth and carbon mineralization. We further noted that cells with a higher DNA content seemed to be particularly abundant in the light treatments at the end of the incubation (Fig. S3 showing higher proportions of MNA and HNA populations at 18 d). A taxonomic characterization of these bacterial populations appearing on the cytograms (using a cell sorter for example, see Fig. S4) is needed to better understand the effects of sunlight on the bacterial cycling of permafrost carbon and composition structure of the communities.

4.5 Significance at the lake scale

The strong impact of sunlight reported here needs to be considered in the specific context of thermokarst lakes. In such humic lakes, only surface layers receive photochemically active photons. For example, Vähätalo et al. (2000) calculated that 90 % of photomineralization happened in the top 1 m of a humic lake, with UV radiation contributing to 77 % of this mineralization. Similarly, the study from Koehler et al. (2014) based on 1086 Swedish lakes concluded that 95 % of the depth-integrated DIC photoproduction happened in the upper 0.8 m of the water column. Attenuation coefficients were estimated from downwelling irradiance profiles realized in SAS2A in August 2016 (unpublished data) with a multispectral radiometer (Satlantic Inc., now owned by Seabird Scientific). In July, 90 % of incident photons were attenuated at 5, 14 and 23 cm for wavelengths 380, 443 and 491 nm, respectively. This is considerably shallower than the photoactive depth mentioned above for Swedish lakes, but it is important to note that our study lake is extremely humic by comparison to the majority of the lakes in the database used by Koehler et al. (2014): only 25 % have an absorption coefficient at 305 nm above 89 m^{-1}, against a value of 143 m^{-1} for SAS2A lake at T_0. Therefore, most of direct photomineralization in SAS2A is occurring in the first centimeters of the water column. In our experiment, degradation was constrained to a 7.3 cm depth (diameter of bottles floating under a thin layer of transparent tap water), which makes it representative of a typical exposure at the very surface of the lake. Previous studies indicated that thermokarst lakes in this area are strongly stratified most of the year, with brief mixing periods in spring and autumn which depend on lake morphology (Matveev et al., 2019). Notably, the small size of these lakes and their high DOM content impede on a complete spring turnover, where only top layers get mixed for a few days until summer stratification is established. Partial mixing then occurs on a daily basis at night. This mixing regime generates conditions where sunlight can only reach surface layers, but partial mixing at night likely brings fresh DOM to the surface on a diurnal basis. Thus, the experimental exposure of the same DOM molecules for 18 d may have underestimated the photodegradation potentially taking place in situ, where substrate limitation is less likely to occur. We

indeed observed the plateauing of certain proxies (e.g., DIC, bacterial growth in L treatment), suggesting the limitation of certain substrates in the absence of mixing renewal.

Finally, the study by Deshpande et al. (2016) highlighted the importance of attached bacteria in SAS2A lake, where more than 70 % of BA and BP was associated to particles larger than 3 µm. As most particles were removed in the present experiment (filtration either through 1.5 or 0.2 µm), it is likely that bacterioplankton respiration, growth and DOM degradation were underestimated. Moreover, our experiment provides information on DOM biodegradation potentially happening in the upper oxygenated layers, but it does not address bacterial activity in deeper anoxic layers of the lake. To fully account for the importance of dark bacterial mineralization relative to photomineralization, experiments will have to include particle-attached flora and respect the anoxic conditions prevailing in these systems. The present study can only underline that photomineralization is an efficient process accelerating DOM processing in epilimnetic waters of thermokarst lakes.

5 Conclusions

Our work suggests that winter DOM collected from a thermokarst lake in a subarctic peatland has a high potential of photoreactivity at ice-off, and that the bacterial community originating from the water was strongly stimulated by sunlight. About $5.0 \, \text{mgC L}^{-1}$ (23 % of initial DOC concentration) was lost over 18 d when bacteria and sunlight were both at play. Results indicate that (1) direct effects of sunlight (78 % of this DOC loss) were much larger than indirect effects (22 % of the DOC loss, stimulation of bacterial consumption through the synthesis of labile photoproducts), (2) photomineralization (CO_2 production by direct or indirect effects) accounted for a maximum of 51 % of the DOC losses (~ 10 % of initial DOC concentration), and (3) most of the remaining DOC loss was likely associated to photoflocculation. The positive effect of sunlight on the bacterial community was particularly demonstrated by the outstanding regrowth of the population left in L treatment (even after the 0.2 µm filtration). Without sunlight stimulation, no detectable DOC or CDOM losses could be attributed to the sole action of bacteria, yet they remained relatively active in the dark and produced FDOM. The highly colored aromatic DOM found in these lakes at the end of winter was quite refractory to biodegradation but particularly sensitive to sunlight. Our work thus suggests that sunlight is an important mediator of CO_2 emission and carbon burial in peatland thermokarst lakes after the ice cover melts. The next step will be to quantify this cycling at the lake scale by taking into account the natural conditions prevailing in spring, including local irradiance, temperature and oxygen concentration. A direct quantification of DOM flocculation and its mediation by sunlight are also needed. Finally, the inclusion of particle-attached

microorganisms and the characterization of bacterial communities during this seasonal transition (from dark anoxic conditions under the ice cover to varying exposure to sunlight and oxygen in the diurnally mixed surface layer of the lake) would help to improve our understanding of climate change effects on the carbon cycling in this important class of lakes.

Review statement. This paper was edited by Helge Niemann and reviewed by Brent Dalzell and one anonymous referee.

References

Adams, H. E., Crump, B. C., and Kling, G. W.: Temperature controls on aquatic bacterial production and community dynamics in arctic lakes and streams, Environ. Microbiol., 12, 1319–1333, https://doi.org/10.1111/j.1462-2920.2010.02176.x, 2010.

Arlen-Pouliot, Y. and Bhiry, N.: Palaeoecology of a palsa and a filled thermokarst pond in a permafrost peatland, subarctic Québec, Canada, The Holocene, 15, 408–419, https://doi.org/10.1191/0959683605hl818rp, 2005.

Bégin, P. N. and Vincent, W. F.: Permafrost thaw lakes and ponds as habitats for abundant rotifer populations, Arct. Sci., 3, 354–377, https://doi.org/10.1139/as-2016-0017, 2017.

Berggren, M., Laudon, H., and Jansson, M.: Landscape regulation of bacterial growth efficiency in boreal freshwaters, Global Biogeochem. Cy., 21, GB4002, https://doi.org/10.1029/2006GB002844, 2007.

Berggren, M., Gudasz, C., Guillemette, F., Hensgens, G., Ye, L., and Karlsson, J.: Systematic microbial production of optically active dissolved organic matter in subarctic lake water, Limnol. Oceanogr., 65, 951–961, https://doi.org/10.1002/lno.11362, 2020.

Bertilsson, S., Burgin, A., Carey, C. C., Fey, S. B., Grossart, H. P., Grubisic, L. M., Jones, I. D., Kirillin, G., Lennon, J. T., Shade, A., and Smyth, R. L.: The under-ice microbiome of seasonally frozen lakes, Limnol. Oceanogr., 58, 1998–2012, https://doi.org/10.4319/lo.2013.58.6.1998, 2013.

Bhiry, N., Delwaide, A., Allard, M., Bégin, Y., Filion, L., Lavoie, M., Nozais, C., Payette, S., Pienitz, R., Saulnier-Talbot, É., and Vincent, W. F.: Environmental change in the Great Whale River region, Hudson Bay: Five decades of multidisciplinary research by Centre d'études nordiques (CEN), Écoscience, 18, 182–203, https://doi.org/10.2980/18-3-3469, 2011.

Biskaborn, B. K., Smith, S. L., Noetzli, J., Matthes, H., Vieira, G., Streletskiy, D. A., Schoeneich, P., Romanovsky, V. E., Lewkowicz, A. G., Abramov, A., Allard, M., Boike, J., Cable, W. L., Christiansen, H. H., Delaloye, R., Diekmann, B., Drozdov, D., Etzelmüller, B., Grosse, G., Guglielmin, M., Ingeman-Nielsen, T., Isaksen, K., Ishikawa, M., Johansson, M., Johannsson, H., Joo, A., Kaverin, D., Kholodov, A., Konstantinov, P., Kröger, T., Lambiel, C., Lanckman, J. P., Luo, D., Malkova, G., Meiklejohn, I., Moskalenko, N., Oliva, M., Phillips, M., Ramos, M., Sannel, A. B. K., Sergeev, D., Seybold, C., Skryabin, P., Vasiliev, A., Wu, Q., Yoshikawa, K., Zheleznyak, M., and Lantuit, H.: Permafrost is warming at a global scale, Nat. Commun., 10, 1–11, https://doi.org/10.1038/s41467-018-08240-4, 2019.

Bižić-Ionescu, M., Amann, R., and Grossart, H. P.: Massive regime shifts and high activity of heterotrophic bacteria in an ice-covered lake, PLoS One, 9, 1–17, https://doi.org/10.1371/journal.pone.0113611, 2014.

Block, B. D., Denfeld, B. A., Stockwell, J. D., Flaim, G., Grossart, H. P. F., Knoll, L. B., Maier, D. B., North, R. L., Rautio, M., Rusak, J. A., Sadro, S., Weyhenmeyer, G. A., Bramburger, A. J., Branstrator, D. K., Salonen, K., and Hampton, S. E.: The unique methodological challenges of winter limnology, Limnol. Oceanogr. Method., 17, 42–57, https://doi.org/10.1002/lom3.10295, 2019.

CEN (Centre for northern studies): Climate station data from Whapmagoostui-Kuujjuarapik Region in Nunavik, Quebec, Canada, v. 1.5 (1987–2019), Nordicana D4, https://doi.org/10.5885/45057SL-EADE4434146946A7, 2020.

Cole, J. J., Prairie, Y. T., Caraco, N. F., McDowell, W. H., Tranvik, L. J., Striegl, R. G., Duarte, C. M., Kortelainen, P., Downing, J. A., Middelburg, J. J., and Melack, J.: Plumbing the Global Carbon Cycle: Integrating Inland Waters into the Terrestrial Carbon Budget, Ecosystems, 10, 172–185, https://doi.org/10.1007/s10021-006-9013-8, 2007.

Cory, R. M., Crump, B. C., Dobkowski, J. A., and Kling, G. W.: Surface exposure to sunlight stimulates CO_2 release from permafrost soil carbon in the Arctic, P. Natl. Acad. Sci. USA, 110, 3429–3434, https://doi.org/10.1073/pnas.1214104110, 2013.

Cory, R. M. and Kling, G. W.: Interactions between sunlight and microorganisms influence dissolved organic matter degradation along the aquatic continuum, Limnol. Oceanogr. Lett., 3, 102–116, https://doi.org/10.1002/lol2.10060, 2018.

Dean, J. F., van Hal, J. R., Dolman, A. J., Aerts, R., and Weedon, J. T.: Filtration artefacts in bacterial community composition can affect the outcome of dissolved organic matter biolability assays, Biogeosciences, 15, 7141–7154, https://doi.org/10.5194/bg-15-7141-2018, 2018.

del Giorgio, P. A. and Bouvier, T. C.: Linking the physiologic and phylogenetic successions in free-living bacterial communities along an estuarine salinity gradient, Limnol. Oceanogr., 47, 471–486, https://doi.org/10.4319/lo.2002.47.2.0471, 2002.

Denfeld, B. A., Baulch, H. M., del Giorgio, P. A., Hampton, S. E., and Karlsson, J.: A synthesis of carbon dioxide and methane dynamics during the ice-covered period of northern lakes, Limnol. Oceanogr. Lett., 3, 117–131, https://doi.org/10.1002/lol2.10079, 2018.

Deshpande, B. N., Crevecoeur, S., Matveev, A., and Vincent, W. F.: Bacterial production in subarctic peatland lakes enriched by thawing permafrost, Biogeosciences, 13, 4411–4427, https://doi.org/10.5194/bg-13-4411-2016, 2016.

Elder, C. D., Xu, X., Walker, J., Schnell, J. L., Hinkel, K. M., Townsend-Small, A., Arp, C. D., Pohlman, J. W., Gaglioti, B. V., and Czimczik, C. I.: Greenhouse gas emissions from diverse Arctic Alaskan lakes are dominated by young carbon, Nat. Clim. Change, 8, 166–171, https://doi.org/10.1038/s41558-017-0066-9, 2018.

Faust, D. R. and Liebig, M. A.: Effects of storage time and temperature on greenhouse gas samples in Exetainer vials with chlorobutyl septa caps, MethodsX, 5, 857–864, https://doi.org/10.1016/j.mex.2018.06.016, 2018.

Folhas, D., Duarte, A. C., Pilote, M., Vincent, W. F., Freitas, P., Vieira, G., Silva, A. M. S., Duarte, R. M. B. O., and Canário, J.: Structural characterization of dissolved organic matter in permafrost peatland lakes, Water, 12, 3059, https://doi.org/10.3390/w12113059, 2020.

Gao, H. and Zepp, R. G.: Factors Influencing Photoreactions of Dissolved Organic Matter in a Coastal River of the Southeastern United States, Environ. Sci. Technol., 32, 2940–2946, https://doi.org/10.1021/es9803660, 1998.

Girard, C., Langlois, V., Vigneron, A., Vincent, W. F., and Culley, A. I.: Seasonal Regime Shift in the Viral Com-

munities of a Permafrost Thaw Lake, Viruses, 12, 1204, https://doi.org/10.3390/v12111204, 2020.

Granéli, W., Lindell, M., and Tranvik, L.: Photo-oxidative production of dissolved inorganic carbon in lakes of different humic content, Limnol. Oceanogr., 41, 698–706, https://doi.org/10.4319/lo.1996.41.4.0698, 1996.

Groeneveld, M., Tranvik, L., Natchimuthu, S., and Koehler, B.: Photochemical mineralisation in a boreal brown water lake: Considerable temporal variability and minor contribution to carbon dioxide production, Biogeosciences, 13, 3931–3943, https://doi.org/10.5194/bg-13-3931-2016, 2016.

Guillemette, F., von Wachenfeldt, E., Kothawala, D. N., Bastviken, D., and Tranvik, L. J.: Preferential sequestration of terrestrial organic matter in boreal lake sediments, J. Geophys. Res.-Biogeo., 122, 863–874, https://doi.org/10.1002/2016JG003735, 2017.

Hampton, S. E., Galloway, A. W. E., Powers, S. M., Ozersky, T., Woo, K. H., Batt, R. D., Labou, S. G., O'Reilly, C. M., Sharma, S., Lottig, N. R., Stanley, E. H., North, R. L., Stockwell, J. D., Adrian, R., Weyhenmeyer, G. A., Arvola, L., Baulch, H. M., Bertani, I., Bowman, L. L., Carey, C. C., Catalan, J., Colom-Montero, W., Domine, L. M., Felip, M., Granados, I., Gries, C., Grossart, H.-P., Haberman, J., Haldna, M., Hayden, B., Higgins, S. N., Jolley, J. C., Kahilainen, K. K., Kaup, E., Kehoe, M. J., MacIntyre, S., Mackay, A. W., Mariash, H. L., McKay, R. M., Nixdorf, B., Nõges, P., Nõges, T., Palmer, M., Pierson, D. C., Post, D. M., Pruett, M. J., Rautio, M., Read, J. S., Roberts, S. L., Rücker, J., Sadro, S., Silow, E. A., Smith, D. E., Sterner, R. W., Swann, G. E. A., Timofeyev, M. A., Toro, M., Twiss, M. R., Vogt, R. J., Watson, S. B., Whiteford, E. J., and Xenopoulos, M. A.: Ecology under lake ice, edited by: Grover, J., Ecol. Lett., 20, 98–111, https://doi.org/10.1111/ele.12699, 2017.

Helms, J. R., Stubbins, A., Ritchie, J. D., Minor, E. C., Kieber, D. J., and Mopper, K.: Absorption spectral slopes and slope ratios as indicators of molecular weight, source, and photobleaching of chromophoric dissolved organic matter, Limnol. Oceanogr., 53, 955–969, https://doi.org/10.4319/lo.2008.53.3.0955, 2008.

Helms, J. R., Mao, J., Schmidt-Rohr, K., Abdulla, H., and Mopper, K.: Photochemical flocculation of terrestrial dissolved organic matter and iron, Geochim. Cosmochim. Ac., 121, 398–413, https://doi.org/10.1016/j.gca.2013.07.025, 2013.

Hughes-Allen, L., Bouchard, F., Laurion, I., Séjourné, A., Marlin, C., Hatté, C., Costard, F., Fedorov, A., and Desyatkin, A.: Seasonal patterns in greenhouse gas emissions from thermokarst lakes in Central Yakutia (Eastern Siberia), Limnol. Oceanogr., 6, S98–S116, https://doi.org/10.1002/lno.11665, 2021.

Jansen, J., Thornton, B. F., Jammet, M. M., Wik, M., Cortés, A., Friborg, T., MacIntyre, S., and Crill, P. M.: Climate-Sensitive Controls on Large Spring Emissions of CH_4 and CO_2 From Northern Lakes, J. Geophys. Res.-Biogeo., 124, 2379–2399, https://doi.org/10.1029/2019JG005094, 2019.

Kirchman, D., K'nees, E., and Hodson, R.: Leucine incorporation and its potential as a measure of protein synthesis by bacteria in natural aquatic systems, Appl. Environ. Microbiol., 49, 599–607, 1985.

Koehler, B., Landelius, T., Weyhenmeyer, G. A., Machida, N., and Tranvik, L. J.: Sunlight-induced carbon dioxide emissions from inland waters, Global Biogeochem. Cy., 28, 696–711, https://doi.org/10.1002/2014GB004850, 2014.

Lapierre, J. F., Guillemette, F., Berggren, M., and del Giorgio, P. A.: Increases in terrestrially derived carbon stimulate organic carbon processing and CO_2 emissions in boreal aquatic ecosystems, Nat. Commun., 4, 2972, https://doi.org/10.1038/ncomms3972, 2013.

Laurion, I., Massicotte, P., Mazoyer, F., Negandhi, K., and Mladenov, N.: Weak mineralization despite strong processing of dissolved organic matter in Eastern Arctic tundra ponds, Limnol. Oceanogr., 66, S47–S63, https://doi.org/10.1002/lno.11634, 2021.

Logozzo, L., Tzortziou, M., Neale, P., and Clark, J. B.: Photochemical and Microbial Degradation of Chromophoric Dissolved Organic Matter Exported From Tidal Marshes, J. Geophys. Res.-Biogeo., 126, 1–24, https://doi.org/10.1029/2020JG005744, 2021.

Matveev, A., Laurion, I., Deshpande, B. N., Bhiry, N., and Vincent, W. F.: High methane emissions from thermokarst lakes in subarctic peatlands, Limnol. Oceanogr., 61, S150–S164, https://doi.org/10.1002/lno.10311, 2016.

Matveev, A., Laurion, I., and Vincent, W. F.: Winter Accumulation of Methane and its Variable Timing of Release from Thermokarst Lakes in Subarctic Peatlands, J. Geophys. Res.-Biogeo., 124, 3521–3535, https://doi.org/10.1029/2019JG005078, 2019.

Mazoyer, F., Laurion, I., and Rautio, M.: Dissolved organic matter and bacterial data, along with associated temperature-irradiance metadata for a degradation experiment using winter water from a subarctic thermokarstic peatland lake in Nunavik, Québec, Canada, v. 1.0 (2016–2016), Nordicana D97 [data set], https://doi.org/10.5885/45759CE-9ED4BB6AE585446C, 2022.

Mopper, K., Kieber, D. J., and Stubbins, A.: Marine Photochemistry of Organic Matter: Processes and Impacts, in: Biogeochemistry of Marine Dissolved Organic Matter, edited by: Hansell, D. A. and Carlson, C. A., 389–450, Elsevier, https://doi.org/10.1016/B978-0-12-405940-5.00008-X, 2015.

Moran, M. A. and Zepp, R. G.: Role of photoreactions in the formation of biologically labile compounds from dissolved organic matter, Limnol. Oceanogr., 42, 1307–1316, https://doi.org/10.4319/lo.1997.42.6.1307, 1997.

Moran, M. A., Sheldon, W. M., and Zepp, R. G.: Carbon loss and optical property changes during long-term photochemical and biological degradation of estuarine dissolved organic matter, Limnol. Oceanogr., 45, 1254–1264, https://doi.org/10.4319/lo.2000.45.6.1254, 2000.

Mostovaya, A., Hawkes, J. A., Koehler, B., Dittmar, T., and Tranvik, L. J.: Emergence of the Reactivity Continuum of Organic Matter from Kinetics of a Multitude of Individual Molecular Constituents, Environ. Sci. Technol., 51, 11571–11579, https://doi.org/10.1021/acs.est.7b02876, 2017.

Murphy, K. R., Butler, K. D., Spencer, R. G. M., Stedmon, C. A., Boehme, J. R., and Aiken, G. R.: Measurement of Dissolved Organic Matter Fluorescence in Aquatic Environments: An Interlaboratory Comparison, Environ. Sci. Technol., 44, 9405–9412, https://doi.org/10.1021/es102362t, 2010.

Murphy, K. R., Stedmon, C. A., Graeber, D., and Bro, R.: Fluorescence spectroscopy and multi-way techniques, PARAFAC, Anal. Methods, 5, 6557, https://doi.org/10.1039/c3ay41160e, 2013.

Murphy, K. R., Stedmon, C. A., Wenig, P., and Bro, R.: OpenFluor – an online spectral library of auto-fluorescence by organic compounds in the environment, Anal. Methods, 6, 658–661, https://doi.org/10.1039/C3AY41935E, 2014.

Murphy, K. R., Timko, S. A., Gonsior, M., Powers, L. C., Wünsch, U. J., and Stedmon, C. A.: Photochemistry Illuminates Ubiquitous Organic Matter Fluorescence Spectra, Environ. Sci. Technol., 52, 11243–11250, https://doi.org/10.1021/acs.est.8b02648, 2018.

Obernosterer, I. and Benner, R.: Competition between biological and photochemical processes in the mineralization of dissolved organic carbon, Limnol. Oceanogr., 49, 117–124, https://doi.org/10.4319/lo.2004.49.1.0117, 2004.

Olefeldt, D., Goswami, S., Grosse, G., Hayes, D., Hugelius, G., Kuhry, P., McGuire, A. D., Romanovsky, V. E., Sannel, A. B. K., Schuur, E. A. G., and Turetsky, M. R.: Circumpolar distribution and carbon storage of thermokarst landscapes, Nat. Commun., 7, 13043, https://doi.org/10.1038/ncomms13043, 2016.

Oleinikova, O. V., Drozdova, O. Y., Lapitskiy, S. A., Demin, V. V., Bychkov, A. Y., and Pokrovsky, O. S.: Dissolved organic matter degradation by sunlight coagulates organo-mineral colloids and produces low-molecular weight fraction of metals in boreal humic waters, Geochim. Cosmochim. Ac., 211, 97–114, https://doi.org/10.1016/j.gca.2017.05.023, 2017.

Osburn, C. L., Handsel, L. T., Mikan, M. P., Paerl, H. W., and Montgomery, M. T.: Fluorescence Tracking of Dissolved and Particulate Organic Matter Quality in a River-Dominated Estuary, Environ. Sci. Technol., 46, 8628–8636, https://doi.org/10.1021/es3007723, 2012.

Pickard, A. E., Heal, K. V., McLeod, A. R., and Dinsmore, K. J.: Temporal changes in photoreactivity of dissolved organic carbon and implications for aquatic carbon fluxes from peatlands, Biogeosciences, 14, 1793–1809, https://doi.org/10.5194/bg-14-1793-2017, 2017.

Porcal, P., Dillon, P. J., and Molot, L. A.: Temperature Dependence of Photodegradation of Dissolved Organic Matter to Dissolved Inorganic Carbon and Particulate Organic Carbon, edited by: Almeida, A., PLoS One, 10, e0128884, https://doi.org/10.1371/journal.pone.0128884, 2015.

Prėskienis, V., Laurion, I., Bouchard, F., Douglas, P. M. J., Billett, M. F., Fortier, D., and Xu, X.: Seasonal patterns in greenhouse gas emissions from lakes and ponds in a High Arctic polygonal landscape, Limnol. Oceanogr., 66, S117–S141, https://doi.org/10.1002/lno.11660, 2021.

Przytulska, A., Comte, J., Crevecoeur, S., Lovejoy, C., Laurion, I., and Vincent, W. F.: Phototrophic pigment diversity and picophytoplankton in permafrost thaw lakes, Biogeosciences, 13, 13–26, https://doi.org/10.5194/bg-13-13-2016, 2016.

Pullin, M. J., Bertilsson, S., Goldstone, J. V., and Voelker, B. M.: Effects of sunlight and hydroxyl radical on dissolved organic matter: Bacterial growth efficiency and production of carboxylic acids and other substrates, Limnol. Oceanogr., 49, 2011–2022, https://doi.org/10.4319/lo.2004.49.6.2011, 2004.

Roiha, T., Laurion, I., and Rautio, M.: Carbon dynamics in highly heterotrophic subarctic thaw ponds, Biogeosciences, 12, 7223–7237, https://doi.org/10.5194/bg-12-7223-2015, 2015.

Rösel, S., Allgaier, M., and Grossart, H. P.: Long-Term Characterization of Free-Living and Particle-Associated Bacterial Communities in Lake Tiefwaren Reveals Distinct Seasonal Patterns, Microb. Ecol., 64, 571–583, https://doi.org/10.1007/s00248-012-0049-3, 2012.

Schuur, E. A. G., McGuire, A. D., Schädel, C., Grosse, G., Harden, J. W., Hayes, D. J., Hugelius, G., Koven, C. D., Kuhry, P., Lawrence, D. M., Natali, S. M., Olefeldt, D., Romanovsky, V. E., Schaefer, K., Turetsky, M. R., Treat, C. C., and Vonk, J. E.: Climate change and the permafrost carbon feedback, Nature, 520, 171–179, https://doi.org/10.1038/nature14338, 2015.

Sepulveda-Jauregui, A., Walter Anthony, K. M., Martinez-Cruz, K., Greene, S., and Thalasso, F.: Methane and carbon dioxide emissions from 40 lakes along a north-south latitudinal transect in Alaska, Biogeosciences, 12, 3197–3223, https://doi.org/10.5194/bg-12-3197-2015, 2015.

Shirokova, L. S., Chupakov, A. V., Zabelina, S. A., Neverova, N. V., Payandi-Rolland, D., Causserand, C., Karlsson, J., and Pokrovsky, O. S.: Humic surface waters of frozen peat bogs (permafrost zone) are highly resistant to bio- and photodegradation, Biogeosciences, 16, 2511–2526, https://doi.org/10.5194/bg-16-2511-2019, 2019.

Shirokova, L. S., Chupakov, A. V., Ivanova, I. S., Moreva, O. Y., Zabelina, S. A., Shutskiy, N. A., Loiko, S. V., and Pokrovsky, O. S.: Lichen, moss and peat control of C, nutrient and trace metal regime in lakes of permafrost peatlands, Sci. Total Environ., 782, 146737, https://doi.org/10.1016/j.scitotenv.2021.146737, 2021.

Smith, D. and Azam, F.: A simple, economical method for measuring bacterial protein synthesis rates in seawater using ^{3}H-leucine, Mar. Microb. Food Webs, 6, 107–114, 1992.

Sobek, S., Tranvik, L. J., and Cole, J. J.: Temperature independence of carbon dioxide supersaturation in global lakes, Global Biogeochem. Cy., 19, GB2003, https://doi.org/10.1029/2004GB002264, 2005.

Søndergaard, M., Stedmon, C. A., and Borch, N. H.: Fate of terrigenous dissolved organic matter (DOM) in estuaries: Aggregation and bioavailability, Ophelia, 57, 161–176, https://doi.org/10.1080/00785236.2003.10409512, 2003.

Stedmon, C. A. and Bro, R.: Characterizing dissolved organic matter fluorescence with parallel factor analysis: a tutorial, Limnol. Oceanogr. Method., 6, 572–579, 2008.

Stedmon, C. A., Markager, S., and Bro, R.: Tracing dissolved organic matter in aquatic environments using a new approach to fluorescence spectroscopy, Mar. Chem., 82, 239–254, https://doi.org/10.1016/S0304-4203(03)00072-0, 2003.

Stubbins, A., Hubbard, V., Uher, G., Law, C. S., Upstill-Goddard, R. C., Aiken, G. R., and Mopper, K.: Relating Carbon Monoxide Photoproduction to Dissolved Organic Matter Functionality, Environ. Sci. Technol., 42, 3271–3276, https://doi.org/10.1021/es703014q, 2008.

Tank, S. E., Vonk, J. E., Walvoord, M. A., McClelland, J. W., Laurion, I., and Abbott, B. W.: Landscape matters: Predicting the biogeochemical effects of permafrost thaw on aquatic networks with a state factor approach, Permafrost Periglac., 31, 358–370, https://doi.org/10.1002/ppp.2057, 2020.

Tranvik, L. J., Downing, J. A., Cotner, J. B., Loiselle, S. A., Striegl, R. G., Ballatore, T. J., Dillon, P., Finlay, K., Fortino, K., Knoll, L. B., Kortelainen, P. L., Kutser, T., Larsen, S., Laurion, I., Leech, D. M., Leigh McCallister, S., McKnight, D. M., Melack, J. M., Overholt, E., Porter, J. A., Prairie, Y., Renwick, W. H., Roland, F., Sherman, B. S., Schindler, D. W., Sobek, S., Tremblay, A., Vanni, M. J., Verschoor, A. M., Von Wachenfeldt, E., and Weyhenmeyer, G. A.: Lakes and reservoirs as regulators of carbon cycling and climate, Limnol. Oceanogr., 54, 2298–2314, https://doi.org/10.4319/lo.2009.54.6_part_2.2298, 2009.

Turetsky, M. R.: The Role of Bryophytes in Carbon and Nitrogen Cycling, Bryologist, 106, 395–409, 2003.

Vachon, D., Lapierre, J., and del Giorgio, P. A.: Seasonality of photochemical dissolved organic carbon mineralization and its relative contribution to pelagic CO_2 production in northern lakes, J. Geophys. Res.-Biogeo., 121, 864–878, https://doi.org/10.1002/2015JG003244, 2016.

Vachon, D., Solomon, C. T., and del Giorgio, P. A.: Reconstructing the seasonal dynamics and relative contribution of the major processes sustaining CO_2 emissions in northern lakes, Limnol. Oceanogr., 62, 706–722, https://doi.org/10.1002/lno.10454, 2017.

Vähätalo, A. V. and Wetzel, R. G.: Long-term photochemical and microbial decomposition of wetland-derived dissolved organic matter with alteration of $^{13}C : {}^{12}C$ mass ratio, Limnol. Oceanogr., 53, 1387–1392, https://doi.org/10.4319/lo.2008.53.4.1387, 2008.

Vähätalo, A. V., Salkinoja-Salonen, M., Taalas, P., and Salonen, K.: Spectrum of the quantum yield for photochemical mineralization of dissolved organic carbon in a humic lake, Limnol. Oceanogr., 45, 664–676, https://doi.org/10.4319/lo.2000.45.3.0664, 2000.

Vähätalo, A. V., Salonen, K. M., and Wetzel, R. G.: Photochemical transformation of allochthonous organic matter provides bioavailable nutrients in a humic lake, Arch. Hydrobiol., 156, 287–314, https://doi.org/10.1127/0003-9136/2003/0156-0287, 2003.

Vincent, W. F., Lemay, M., and Allard, M.: Arctic permafrost landscapes in transition: towards an integrated Earth system approach, Arct. Sci., 3, 39–64, https://doi.org/10.1139/as-2016-0027, 2017.

Vonk, J. E., Tank, S. E., Mann, P. J., Spencer, R. G. M., Treat, C. C., Striegl, R. G., Abbott, B. W., and Wickland, K. P.: Biodegradability of dissolved organic carbon in permafrost soils and aquatic systems: A meta-analysis, Biogeosciences, 12, 6915–6930, https://doi.org/10.5194/bg-12-6915-2015, 2015a.

Vonk, J. E., Tank, S. E., Bowden, W. B., Laurion, I., Vincent, W. F., Alekseychik, P., Amyot, M., Billet, M. F., Canário, J., Cory, R. M., Deshpande, B. N., Helbig, M., Jammet, M., Karlsson, J., Larouche, J., MacMillan, G., Rautio, M., Walter Anthony, K. M., and Wickland, K. P.: Reviews and syntheses: Effects of permafrost thaw on Arctic aquatic ecosystems, Biogeosciences, 12, 7129–7167, https://doi.org/10.5194/bg-12-7129-2015, 2015b.

von Wachenfeldt, E. and Tranvik, L. J.: Sedimentation in Boreal Lakes – The Role of Flocculation of Allochthonous Dissolved Organic Matter in the Water Column, Ecosystems, 11, 803–814, https://doi.org/10.1007/s10021-008-9162-z, 2008.

von Wachenfeldt, E., Sobek, S., Bastviken, D., and Tranvik, L. J.: Linking allochthonous dissolved organic matter and boreal lake sediment carbon sequestration: The role of light-mediated flocculation, Limnol. Oceanogr., 53, 2416–2426, https://doi.org/10.4319/lo.2008.53.6.2416, 2008.

von Wachenfeldt, E., Bastviken, D., and Tranvika, L. J.: Microbially induced flocculation of allochthonous dissolved organic carbon in lakes, Limnol. Oceanogr., 54, 1811–1818, https://doi.org/10.4319/lo.2009.54.5.1811, 2009.

Ward, C. P., Sleighter, R. L., Hatcher, P. G., and Cory, R. M.: Insights into the complete and partial photooxidation of black carbon in surface waters, Environ. Sci. Process. Im., 16, 721–731, https://doi.org/10.1039/C3EM00597F, 2014.

Ward, C. P., Nalven, S. G., Crump, B. C., Kling, G. W., and Cory, R. M.: Photochemical alteration of organic carbon draining permafrost soils shifts microbial metabolic pathways and stimulates respiration, Nat. Commun., 8, 772, https://doi.org/10.1038/s41467-017-00759-2, 2017.

Weishaar, J. L., Aiken, G. R., Bergamaschi, B. A., Fram, M. S., Fujii, R., and Mopper, K.: Evaluation of Specific Ultraviolet Absorbance as an Indicator of the Chemical Composition and Reactivity of Dissolved Organic Carbon, Environ. Sci. Technol., 37, 4702–4708, https://doi.org/10.1021/es030360x, 2003.

Wetzel, R. G., Hatcher, P. G., and Bianchi, T. S.: Natural photolysis by ultraviolet irradiance of recalcitrant dissolved organic matter to simple substrates for rapid bacterial metabolism, Limnol. Oceanogr., 40, 1369–1380, https://doi.org/10.4319/lo.1995.40.8.1369, 1995.

Wik, M., Varner, R. K., Anthony, K. W., MacIntyre, S., and Bastviken, D.: Climate-sensitive northern lakes and ponds are critical components of methane release, Nat. Geosci., 9, 99–105, https://doi.org/10.1038/ngeo2578, 2016.

Williams, C. J., Yamashita, Y., Wilson, H. F., Jaffe, R., and Xenopoulos, M. A.: Unraveling the role of land use and microbial activity in shaping dissolved organic matter characteristics in stream ecosystems, Limnol. Oceanogr., 55, 1159–1171, https://doi.org/10.4319/lo.2010.55.3.1159, 2010.

Xie, H., Bélanger, S., Song, G., Benner, R., Taalba, A., Blais, M., Tremblay, J.-É., and Babin, M.: Photoproduction of ammonium in the southeastern Beaufort Sea and its biogeochemical implications, Biogeosciences, 9, 3047–3061, https://doi.org/10.5194/bg-9-3047-2012, 2012.